Quest Journals
Journal of Architecture and Civil Engineering
Volume 10 ~ Issue 5 (May 2025) pp: 01-23
ISSN(Online) : 2321-8193
www.questjournals.org

Research Paper

Response Surface Methodology for Evaluating Voids In Metakaolin Modified Granite-Granular Sand Densely Graded Asphalt Concrete

Obazee, Anthony Igunma[1], Ohwerhi, Kelly Erhiferhi[2*]
[1,2] Department of Civil Engineering, University of Port Harcourt, Port Harcourt, Nigeria.
Corresponding Author; Ohwerhi Kelly Erhiferhi,ORCID; 0009-0002-7471-2273

Abstract
This study investigates the optimization of void properties in Metakaolin-Modified Densely Graded Asphalt Concrete (MK-DGAC) using Response Surface Methodology (RSM). The mix includes granite, granular sand, bitumen, and metakaolin (MK) as a pozzolanic additive. Void parameters analyzed are Voids in Mineral Aggregate (VMA), Voids in Total Mix (VTM), and Voids Filled with Bitumen (VFB), which critically influence pavement durability, moisture resistance, and load capacity.Results show that increasing MK content reduces VMA by up to 17.92% (15.67% to 19.09%) and decreases VTM by 61.68% (2.06% to 5.37%), while raising VFB by 21.39% (71.88% to 87.25%). These changes improve binder distribution and moisture resistance but may elevate rutting risk if overdosed. RSM models for VMA and VTM achieved high predictive accuracy with R^2 values of 88.98% and 83.96%, respectively, confirming reliability in capturing void behavior based on granite, sand, bitumen, and MK proportions.Statistical analysis highlights MK as the most influential factor in reducing voids and enhancing bitumen filling, followed by granular sand and bitumen, with granite having minimal impact. The optimized mix proportions identified are approximately 57.3% granite, 32.7% sand, 6.4% bitumen, and 3.63% metakaolin. This formulation yields a VMA of 15.9% (above the 14% minimum), a VTM of 2.03% (slightly below the 3–5% guideline), and a VFB of 86.9% (exceeding typical upper limits), achieving a composite desirability of 96.95%.Overall, the study confirms that carefully dosed metakaolin enhances asphalt concrete void properties, offering a durable, moisture-resistant, and structurally sound pavement mix optimized through RSM coupled with desirability functions.

Keywords; ***Response surface methodology, metakaolin, densely graded asphalt concrete, voids in mineral aggregate, voids in total mix, voids filled with bitumen***

Received 12 May., 2025; Revised 20 May., 2025; Accepted 22 May., 2025 © The author(s) 2025.
Published with open access at ***www.questjournas.org***

I. Introduction

The structural integrity and durability of asphalt concrete pavements are significantly affected by their internal void structure, which plays a key role in determining essential properties such as density, moisture resistance, deformation tolerance, and load support. Densely graded asphalt concrete (DGAC), known for its tightly packed aggregate structure and low air void content, is commonly employed to enhance pavement durability and functionality. Recent studies have highlighted the critical role of air void management in achieving optimal pavement performance. According to Heitzman et al. (2021), both excessive and inadequate air voids can shorten pavement lifespan. Their research, conducted through the National Cooperative Highway Research Program, underscores the need to control air void levels during construction to prevent early deterioration like rutting and cracking. Similarly, Salini and Lenngren (2022) found that DGAC mixes with air voids exceeding 7% are prone to premature failure. They created predictive tools to estimate service life reduction and evaluate potential financial consequences for contractors who fail to meet air void requirements.

Moisture susceptibility is also a critical issue associated with the internal void structure of asphalt mixtures. Higher air void content creates channels that allow water to penetrate the pavement, weakening the bond between the asphalt binder and the aggregate. Sebaaly et al. (2023) observed that mixtures with elevated air void levels tend to have lower tensile strength ratios (TSR), indicating a reduced ability to resist moisture-

related damage. Their findings advocate for the use of engineering-based criteria to assess moisture sensitivity and inform modifications in mix design.

Additionally, deformation resistance, especially in terms of rutting under repeated traffic loads, is closely influenced by the air void content of asphalt mixtures. Zhou et al. (2023) conducted an in-depth review emphasizing the link between air void levels and the permanent deformation behavior of asphalt pavements. Their findings highlight the critical role of proper compaction during construction to manage void content and improve the material's ability to withstand loading. Nevertheless, achieving the ideal air void level becomes increasingly challenging when incorporating supplementary cementitious materials and alternative aggregates into the mix.

Metakaolin, a highly reactive pozzolan produced through the thermal treatment of kaolinite clay, is gaining recognition as a valuable mineral additive in pavement materials. Its ability to enhance mechanical strength, lower permeability, and strengthen the bond between binder and aggregate makes it particularly beneficial. The use of metakaolin in both cementitious and asphalt mixtures supports the increasing emphasis on developing durable and sustainable infrastructure.

In cement-based applications, metakaolin plays a pivotal role in improving the performance of concrete composites. Wei et al. (2024) conducted a comprehensive review on its use in ultra-high-performance concrete (UHPC), emphasizing its effectiveness in boosting compressive strength and minimizing permeability, key factors for long-lasting infrastructure. Similarly, Wang and Zhao (2024) found that grouting materials incorporating metakaolin exhibited enhanced durability in high-temperature geothermal settings, indicating their suitability for demanding construction environments.

The application of metakaolin in asphalt concrete has attracted growing interest in recent years. Yaro et al. (2023) investigated its incorporation into bio-geopolymer-modified asphalt mixtures and observed notable enhancements in rutting resistance, especially under high-temperature conditions. Utilizing response surface methodology (RSM), they identified optimal dosage levels, demonstrating metakaolin's effectiveness in improving resistance to permanent deformation in flexible pavements. These results highlight the material's promise for increasing the durability and resilience of asphalt pavements exposed to heavy traffic and thermal stresses.

Murano et al. (2022) also investigated the use of metakaolin as an additive in hot mix asphalt. Their findings revealed that incorporating metakaolin significantly enhanced the mechanical and volumetric characteristics of the mixture, enabling it to meet standard specifications at optimal binder contents. Notably, they identified 5% nano-metakaolin by asphalt weight as the most effective dosage for improving rheological performance, an essential factor in mitigating pavement distress under diverse service conditions.

Collectively, these studies demonstrate that incorporating metakaolin into both cementitious and asphalt systems leads to significant improvements in structural integrity, moisture resistance, and overall durability. As a result, metakaolin emerges as a highly promising additive for developing sustainable, high-performance pavement materials.

Granite and granular sand have become increasingly popular as aggregate sources in asphalt concrete due to their widespread availability, economic advantages, and strong mechanical performance. However, using them together in mix designs poses specific challenges, particularly in terms of air void content and compaction characteristics. Granite's angular particles provide excellent strength and durability but can hinder compaction because of their interlocking nature. In contrast, granular sand, with its smoother and more rounded particles, enhances workability but may increase air void content if not carefully proportioned with granite (Li & Wang, 2023).

The interaction between granite and granular sand significantly affects air void content, which in turn has a direct impact on the strength and durability of asphalt mixtures. High air void levels can diminish load-bearing capacity and heighten vulnerability to moisture damage, whereas too few air voids may impair workability and hinder effective compaction. Therefore, precise optimization of the aggregate proportions is essential to strike a balance between these competing performance criteria (Chen & Liu, 2022).

To address these challenges, statistical optimization methods like Response Surface Methodology (RSM) and factorial design are being widely used. These techniques facilitate a systematic examination of how different mix variables interact, helping to determine the ideal granite-to-sand ratio for achieving targeted performance outcomes. By applying such optimization strategies, researchers can more accurately predict and manage the influence of aggregate properties on the final concrete characteristics, ensuring the mix satisfies strength, durability, and workability requirements (He & Zhang, 2024).

1.1 Response Surface Methodology

Response Surface Methodology (RSM) is a statistical and mathematical approach commonly used in engineering to model and investigate problems influenced by multiple variables. It aids in optimizing processes by exploring the relationships between input factors and the resulting outcomes. RSM has become a

fundamental tool for optimizing complex systems, enabling researchers to efficiently identify the best operating conditions while minimizing the number of experiments required (Yateh et al., 2023).

RSM uses carefully designed experiments to efficiently investigate the relationships between multiple independent variables and one or more response variables. This approach typically utilizes second-order polynomial models to approximate the actual functional relationships, allowing for the determination of optimal conditions to achieve targeted responses (Zhang et al., 2024). These models are expressed as regression equations and fitted to the experimental data through least squares estimation. As noted by Lamidi et al. (2022), Equation (1) illustrates the general form of the quadratic model applied in RSM.

$$Y = \beta_0 + \sum_{i=1}^{n}(\beta_i z_i) + \sum_{i=1}^{n}(\beta_{ii} z_i^2) + \sum_{i=1}^{n}\sum_{j=1}^{n}(\beta_{ij} z_i z_j) + e \quad (1)$$

Where,Y = response of the experiment,e = the experimental error, β_0 is a constant, β_i is a linear coefficient, β_{ii} is the quadratic coefficient and β_{ij} is the interaction coefficient.

Successful implementation of RSM starts with a carefully planned experimental design. Popular designs include Central Composite Design (CCD) and Box–Behnken Design (BBD), both of which facilitate the creation of accurate predictive models. CCD is especially effective for fitting second-order models by incorporating factorial points, axial points, and center points, while BBD provides an efficient framework for investigating quadratic response surfaces without testing extreme combinations of factors (Onokwai et al., 2022; Megalingam et al., 2023).

After building the regression model, optimization is performed using methods like the steepest ascent approach, desirability functions, or hybrid techniques that incorporate metaheuristics. Desirability functions are particularly useful for multi-response optimization, as they convert multiple response outcomes into a single composite desirability score (Gamero-Salinas & López-Fidalgo, 2024). This helps engineers balance competing goals, such as strength versus cost in material design or efficiency versus safety in process engineering.

RSM has a wide range of practical applications across various engineering fields. In mechanical engineering, Singh et al. (2023) combined RSM with genetic algorithms to optimize the design of high-efficiency prototype vehicles, achieving notable reductions in drag and improvements in fuel efficiency. In materials engineering, Megalingam et al. (2023) utilized RSM to fine-tune production parameters for aluminum 7075 billets, resulting in enhanced structural strength and manufacturing productivity. Environmental engineers also apply RSM to optimize processes such as contaminant removal in water treatment, including the precise dosing of coagulants like polyaluminum chloride (Yateh et al., 2023).

Recent research has emphasized the complementary relationship between RSM and advanced computational methods. For instance, Bbumba et al. (2024) showcased the use of RSM in optimizing adsorption processes, while recognizing the benefits of combining it with artificial intelligence to improve accuracy. Likewise, Lamidi et al. (2022) highlighted the growing practice of integrating RSM with machine learning and simulation tools to achieve more robust optimization in product design and manufacturing systems.

While RSM is highly versatile, it does have limitations. Its dependence on low-order polynomial models can fall short when dealing with highly nonlinear or discontinuous systems. Additionally, the effectiveness of RSM relies heavily on the quality of data and the selection of suitable experimental designs. To overcome these challenges, hybrid approaches that combine RSM with evolutionary algorithms are being developed, offering improved convergence toward global optima in complex engineering problems (Singh et al., 2023; Aje & Adie, 2020).

RSM is increasingly being adopted in food and agricultural engineering as well. For instance, Ismail et al. (2022) utilized RSM to optimize the formulation of an edible bird nest-based instant soup, achieving an optimal balance between nutritional value and sensory appeal. Such varied applications highlight RSM's versatility across both advanced technological fields and consumer-oriented engineering solutions.

Bashash and Saleh Ahari (2025) effectively applied RSM to optimize the mechanical properties of geopolymer concretes incorporating reclaimed asphalt pavement (RAP). Their research showcased RSM's capability to capture the complex interactions within geopolymer mixtures and accurately predict the optimal mix proportions for enhanced mechanical performance.

Similarly, Yaro et al. (2023) utilized RSM to study how asphalt binder content and geopolymer modifiers influence the performance of asphalt concrete. Their work demonstrated RSM's effectiveness in improving predictability and streamlining the design process of asphalt mixtures, resulting in enhanced performance and more precise material selection.

In conclusion, Response Surface Methodology continues to be a vital technique in engineering for the development, enhancement, and optimization of products and processes. By uniting statistical modeling, experimental design, and optimization within a cohesive framework, RSM greatly minimizes the need for extensive trial-and-error testing. As it increasingly integrates with advanced computational methods and algorithms, its importance and effectiveness in addressing contemporary engineering challenges are expected to grow further (Zhang et al., 2024; Bbumba et al., 2024).

In this study, Response Surface Methodology is utilized to assess and optimize the void characteristics of metakaolin-modified densely graded asphalt concrete (DGAC) containing granite dust and granular sand. The main goal is to determine the optimal mix proportions that reduce void content while maintaining the asphalt concrete's structural strength and overall performance. The findings are anticipated to support the creation of more durable, sustainable, and high-performance pavement materials, effectively addressing both environmental and engineering challenges.

II. Materials and Methods

2.1 Materials

This study used well-graded river sand as fine aggregate, with a specific gravity of 2.42 and a fineness modulus of 3.44. Sieve analysis per ASTM C136 (2006) classified the sand as Zone II according to the Unified Soil Classification System, indicating a medium gradation ideal for balancing workability and strength. The relatively high specific gravity and coarser particle size contribute to improved durability, workability, and reduced water demand in concrete mixes. Incorporating this sand into asphalt concrete is expected to enhance structural integrity and extend pavement lifespan.

Granite aggregates with maximum sizes of 12.5 mm, 9 mm, and 6.7 mm were blended and used as coarse aggregate. Prior to use, the aggregates were washed to eliminate dirt and impurities, then air-dried for over 48 hours. A sieve analysis was conducted in accordance with ASTM (2006) standards, classifying the granite as well-graded with a fineness modulus of 3.83. The specific gravity of the granite was determined to be 2.77.

Bitumen with a penetration grade of 60/70 was utilized as the binder in this study. It was obtained from a vendor at the Mile 3 market in Port Harcourt. According to the supplier, the bitumen exhibits the following characteristics: a specific gravity of 1.09, a softening point of 53°C, a penetration value of 68, and a flash point of 250°C.

Metakaolin used in this study was produced by calcining kaolin clay sourced from Aluu, Rivers State. The clay was sun-dried for 48 hours and then heated at 800°C for one hour in a muffle furnace. The resulting metakaolin was ground, sieved through a 75 μm sieve, and analyzed. X-ray fluorescence revealed a high silica content (80.24%) and calcium oxide (4.67%), indicating pozzolanic properties. With a combined acidic oxide content of 91.34%, the material meets BS EN 197-1 (2009) and ASTM C618 (2017) standards for pozzolans. The specific gravity was recorded as 2.52.

2.2 Methods

2.2.1 Preliminary Analysis

Prior to the commencement of the actual or main experimental process, that is, investigating the void properties of metakaolin modified granite-granular sand densely graded asphalt concrete, preliminary investigations were carried out on the unmodified granite-granular sand densely graded asphalt concrete to determine the optimum aggregate blend (OAB) and the optimum bitumen content (OBC).

i. Optimum Aggregate Blend (OAB); To determine the Optimum Aggregate Blend (OAB), the formula-based approach using linear programming was employed, as represented in Equation (2). For multiple sieve sizes, Equation (2) is transformed into a set of equations, as illustrated in Equation (3).

$$aA + bB = P \quad (2)$$

$$\begin{aligned} aA_1 + bB_1 &= P_1 \\ aA_2 + bB_2 &= P_2 \\ aA_3 + bB_3 &= P_3 \\ &\vdots \\ aA_n + bB_n &= P_n \end{aligned} \quad (3)$$

Let $a$and $b$denote the proportions of aggregate sizes A (granite) and B (granular sand), respectively, that pass through a given sieve size. The resulting gradation, P, from the combination of these aggregates must either fall within the limits of the specified job mix formula or be as close as possible to its midpoint, as outlined in Table 1 for flexible pavement wearing courses. A constraint is imposed such that the sum of the optimum proportions a and

b must equal 1. By solving Equation (3) using Microsoft Excel Solver, the optimal blend was determined to be 61.2% for granite (A) and 38.8% for river sand (B), representing the OAB for the unmodified densely graded asphalt concrete.

Table 1. Adopted Job Mix Formula

Sieve size (mm)	19	12.5	9.5	6.3	4.75	2.36	1.18	0.6	0.3	0.15	0.075
JMF (%)	100	86-100	70-90	45-70	40-60	30-52	22-40	16-32	8-9	3-7	0-3

ii Optimum BitumenContent (OBC);The Optimum Bitumen Content (OBC) was determined during the initial wet mix design phase using the conventional Marshall design method, in accordance with ASTM 1559 (2004) as specified by the American Society for Testing and Materials. The bitumen content in the asphalt concrete mixture was limited to a range of 4% to 8% by total mix weight. The previously determined Optimum Aggregate Blend (OAB), comprising 61.2% granite and 38.8% granular sand, was proportionally incorporated into the overall mix design. Based on the findings from the preliminary assessments, the OBC was determined to be 6.42%.

2.2.2 Central Composite Design (CCD) within Response Surface Methodology (RSM)

Initial investigations determined the Optimum Bitumen Content (OBC) for the unmodified densely graded asphalt concrete (DGAC) to be 6.42%. Correspondingly, the Optimum Aggregate Blend (OAB) consisted of 57.27% granite and 36.31% granular sand. For the metakaolin-modified DGAC (MK-DGAC), metakaolin (MK) was incorporated as a mineral filler. Based on standard practices and literature, mineral fillers are typically added at levels ranging from 0% to 10% by the weight of the fine aggregate. Therefore, in designing the MK-DGAC mixes, the fine aggregate fraction (36.31%) identified in the initial stage was adjusted to reflect varying MK proportions. It is assumed that introducing an external additive like MK slightly alters the original DGAC composition. Applying MK at 0–10% of the fine aggregate corresponds to approximately 0–3.63% of the total mix weight. As a result, the granular sand content was varied between 32.68% and 36.31%, while the granite (coarse aggregate) portion was slightly modified to range between 57% and 58% to maintain mix balance. These changes also necessitated a minor adjustment to the bitumen content, which was set between 6.3% and 6.5% of the total mix weight. Using these parameters and constraints, Minitab software generated 31 distinct mix formulations based on a face-centered Central Composite Design (CCD), as presented in Table 2.

Table 2. FC-CCDfor MK-DGAC

RunOrder	Granite (%)	G. Sand (%)	Bitumen (%)	MK (%)
1	57	36.31	6.5	3.63
2	57.5	34.495	6.4	0
3	57.5	34.495	6.4	3.63
4	57	32.68	6.5	0
5	57.5	34.495	6.4	1.815
6	57.5	34.495	6.4	1.815
7	57.5	34.495	6.5	1.815
8	57.5	34.495	6.4	1.815
9	58	36.31	6.5	3.63
10	57	32.68	6.5	3.63
11	57.5	34.495	6.4	1.815
12	57	32.68	6.3	0
13	57.5	32.68	6.4	1.815
14	57.5	34.495	6.4	1.815
15	57.5	34.495	6.4	1.815
16	58	36.31	6.3	0
17	58	34.495	6.4	1.815
18	58	32.68	6.3	3.63
19	58	36.31	6.5	0
20	57.5	34.495	6.3	1.815
21	57.5	34.495	6.4	1.815
22	57.5	36.31	6.4	1.815
23	58	32.68	6.5	3.63
24	57	34.495	6.4	1.815

25	57	36.31	6.3	0
26	57	36.31	6.3	3.63
27	57	36.31	6.5	0
28	58	32.68	6.5	0
29	58	36.31	6.3	3.63
30	58	32.68	6.3	0
31	57	32.68	6.3	3.63

2.2.3 Void Analysis of MK-DGAC

The void characteristics of the MK-DGAC were evaluated through experimental procedures. Specifically, three key parameters were analyzed: Voids in Mineral Aggregate (VMA), which represent the volume of intergranular void space between the aggregate particles in a compacted mix; Voids in Total Mixture (VTM), indicating the total air voids present in the compacted asphalt concrete; and Voids Filled with Bitumen (VFB), which quantify the percentage of VMA that is occupied by bitumen. These properties are critical for assessing the durability, strength, and long-term performance of asphalt mixtures, especially in modified systems such as MK-DGAC, where the introduction of mineral fillers can significantly influence internal void structure and bitumen distribution.

i. MK-DGAC SamplesPreparation; During the preparation of the MK-DGAC specimens, aggregates with incorporation of MK, were weighed based on the CCD proportions outlined in Table 2 and preheated to 180°C. Simultaneously, the bitumen was heated separately to 140°C. Both components were then combined and mixed thoroughly at 180°C until a uniform blend was achieved. The resulting mixture was transferred into a preheated mold and compacted using a Marshall rammer, applying 50 blows on each side at a temperature range of 140°C to 150°C, which is appropriate for pavements subjected to medium traffic loading. Two specimens were produced for each experimental run, resulting in a total of 62 samples.

ii Density-VoidProperties Determination of MK-DGAC Mixtures; The density-voids included measuring the VMA, the VTM, and the VFB. VMA was calculated using Equation (4), VTM was derived using Equation (5), and VFB was determined using Equation (6).

$$VMA = 100 - \frac{G_{bcm} * P_{ta}}{G_{bam}} \quad (4)$$

$$P_{av} = \left(\frac{G_{mm} - G_{bcm}}{G_{mm}}\right) X\ 100 \quad (5)$$

$$VFB = \left(\frac{VMA - P_{av}}{VMA}\right) X\ 100 \quad (6)$$

And;

$$G_{bcm} = \frac{W_a}{W_a - W_w} \quad (7)$$

$$G_{bam} = \frac{P_{ca} + P_{fa}}{\frac{P_{ca}}{G_{bca}} + \frac{P_{fa}}{G_{bfa}}} \quad (8)$$

$$G_{mm} = \frac{P_{ca} + P_{fa} + P_b}{\frac{P_{ca}}{G_{bca}} + \frac{P_{fa}}{G_{bfa}} + \frac{P_b}{G_b}} \quad (9)$$

$$\gamma_{cm} = \frac{W_a}{V_{cm}} \quad (10)$$

Where:

Gbcm refers to the bulk specific gravity of the compacted asphalt specimens;

Gbam denotes the bulk specific gravity of the aggregate blend within the mixture;

Gmm is the maximum specific gravity of the compacted specimens;

$\gamma_{(cm)}$ represents the unit weight of the compacted specimens;

Wa and Ww are the weights of the compacted specimen measured in air and water, respectively;

Pca, Pfa, and Pb indicate the percentage by weight of coarse aggregate, fine aggregate, and bitumen in the mix;

Gbca, Gbfa, and Gb represent the bulk specific gravities of the coarse aggregate (granite), fine aggregate (granular sand), and bitumen, respectively;

Vcm stands for the volume of the compacted specimen.

2.2.4 Response Surface Model for Void Properties Prediction of MK-DGAC

For a four-factor design as employed in this study, Equation (1), becomes;

$$Y = \beta_0 + \beta_1 z_1 + \beta_2 z_2 + \beta_3 z_3 + \beta_4 z_4 + \beta_{11} z_1^2 + \beta_{22} z_2^2 + \beta_{33} z_3^2 + \beta_{44} z_4^2 + \beta_{12} z_1 z_2 + \beta_{13} z_1 z_3 + \beta_{14} z_1 z_4 + \beta_{23} z_2 z_3 + \beta_{24} z_2 z_4 + \beta_{34} z_3 z_4 \quad (11)$$

Where;

Y = responses of modified dense graded asphalt concrete (VMA, VTM, and VFB)
z_1 = proportion of granite in MK-DGAC
z_2 = proportion of granular sand in MK-DGAC
z_3 = proportion of bitumen in MK-DGAC
z_4 = proportion of MK in MK-DGAC
In matrix form, Equation (11) can be represented by Equation (12);

$$Y = [z_i][\beta_i] \quad (12)$$

For n, experimental runs, Equation (12) becomes;

$$Y^n = [(z_i)^n][\beta_i] \quad (13)$$

Where;
$[z_i]$= matrix of the shape function showing interaction between constituents
$[\beta_i]$ = model coefficient matrix
The coefficient vector is represented by Equation (14)

$$[\beta_i] = [\beta_0, \beta_1, \beta_2, \beta_3, \beta_4, \beta_{11}, \beta_{22}, \beta_{33}, \beta_{44}, \beta_{12}, \beta_{13}, \beta_{14}, \beta_{23}, \beta_{24}, \beta_{34}]^T \quad (14)$$

The shape matrix can also be represented by Equation (15).

$$[z_i] = [1, z_1, z_2, z_3, z_4, z_1^2, z_2^2, z_3^2, z_4^2, z_1z_2, z_1z_3, z_1z_4, z_2z_3, z_2z_4, z_3z_4,]^T \quad (15)$$

Multiplying both sides of Equation (13) by a weighting factor, transpose of the shape matrix, yields:

$$[z^n]^T * Y^n = [z^n]^T * [z][\beta_i] \quad (16)$$

Rewriting Equation (16), with introduction of new variables yields;

$$D = [E] * [\beta_i] \quad (17)$$

Where, D and [E] are defined by Equations (18) and (19) respectively;

$$D = [z^n]^T * y^n \quad (18)$$

$$[E] = [z^n]^T * [z^n] \quad (19)$$

From Equation (17);

$$[\beta] = [E]^{-1} * D \quad (20)$$

Equation (20) was used to estimate or determine the coefficients of Equation (11).

2.2.5 Effect Analysis of Components on Voids of MK-DGAC

The influence of various mix components on the void characteristics of MK-DGAC was analyzed through a descriptive statistical approach. The void properties, namely, VMA, VTM, and VFB, were used as the primary response variables. To understand how individual mix constituents (such as bitumen content, granite, granular sand, and metakaolin) and their interactions affect these properties, main effects plots, interaction effects plots, and Pareto charts were employed. The main effects plots provided insight into how changes in each factor independently influenced the void metrics, while interaction plots revealed combined effects between variables. Pareto charts were utilized to rank and visualize the relative significance of each factor and interaction, helping to identify the most influential parameters in controlling void structure within the MK-DGAC mixtures.

2.2.6 Multi-Objectives Optimization of Constituents for Maximum Performance of MK-DGAC

To identify the optimal mix composition for minimizing void-related parameters, namely, VMA and VTM, while maximizing VFB in MK-DGAC, a response optimizer grounded in response surface methodology coupled with desirability function was utilized. This method determines the most effective combination of mix components by ranking potential outcomes based on their desirability scores in descending order. Desirability is a dimensionless value between 0 and 1 that reflects how well a response meets its target; the closer the score is to 1, the nearer the response is to its optimal value.

III. Results and Discussion

3.1 Void Properties Results of MK-DGAC

The void properties of MK-DGAC, as illustrated in Figure 1, demonstrate the substantial influence of metakaolin (MK) content on volumetric parameters including Voids in Mineral Aggregate (VMA), Voids in Total Mix (VTM), and Voids Filled with Bitumen (VFB). These parameters are essential indicators of the structural performance and durability of asphalt mixtures.

The VMA values ranged from 15.669% at run order 29 to 19.090% at run order 12, exhibiting a reduction of up to 17.92% with increasing MK content. According to the Superpave mix design method, the minimum VMA requirements are dependent on the Nominal Maximum Aggregate Size (NMAS): 15.0% for 9.5 mm, 14.0% for 12.5 mm, and 13.0% for 19 mm (Mahoney et al., n.d.). The results in this study satisfy these specifications, indicating that the MK-modified asphalt mixtures maintain an adequate void structure to accommodate binder and resist deformation under loading.

VTM values showed a wide range from 2.0568% at run order 10 to 5.368% at run order 12, reflecting a substantial reduction of up to 61.68% as MK content increased. While this demonstrates MK's ability to densify the asphalt matrix, values falling below 3% may risk bleeding and reduced permeability, while values above 5% could increase air voids and compromise durability. Malaysian specifications recommend an optimal VTM range of 3%–5% to maintain moisture resistance and long-term performance (Fakroun et al., 2021). Thus, fine-tuning the MK dosage is necessary to ensure that VTM remains within the recommended limits.

The VFB, which measures the proportion of VMA filled with binder, ranged from 71.878% to 87.253%, showing an increase of up to 21.39% with higher MK content. This suggests improved binder distribution and enhanced internal cohesion of the asphalt mix. The Superpave design method recommends a VFB range of 65% to 78%, depending on traffic levels (Mahoney et al., n.d.). While the lower value in this study falls within the standard, the upper value exceeds it. High VFB can indicate better moisture resistance but may also result in potential rutting and instability under high-temperature or heavily trafficked conditions.

These findings are consistent with current literature. Shaffie et al. (2022) showed that kaolin clay, like metakaolin, can significantly alter the void structure of hot mix asphalt, improving durability and binder absorption. Similarly, in a study by Fakroun et al. (2021), the inclusion of crumb rubber was found to improve elasticity while affecting VTM and VFB values, confirming the impact of modifiers on volumetric performance. These insights support the potential of MK as an effective mineral additive, capable of enhancing the mechanical behavior of asphalt concrete when incorporated within appropriate dosage limits.

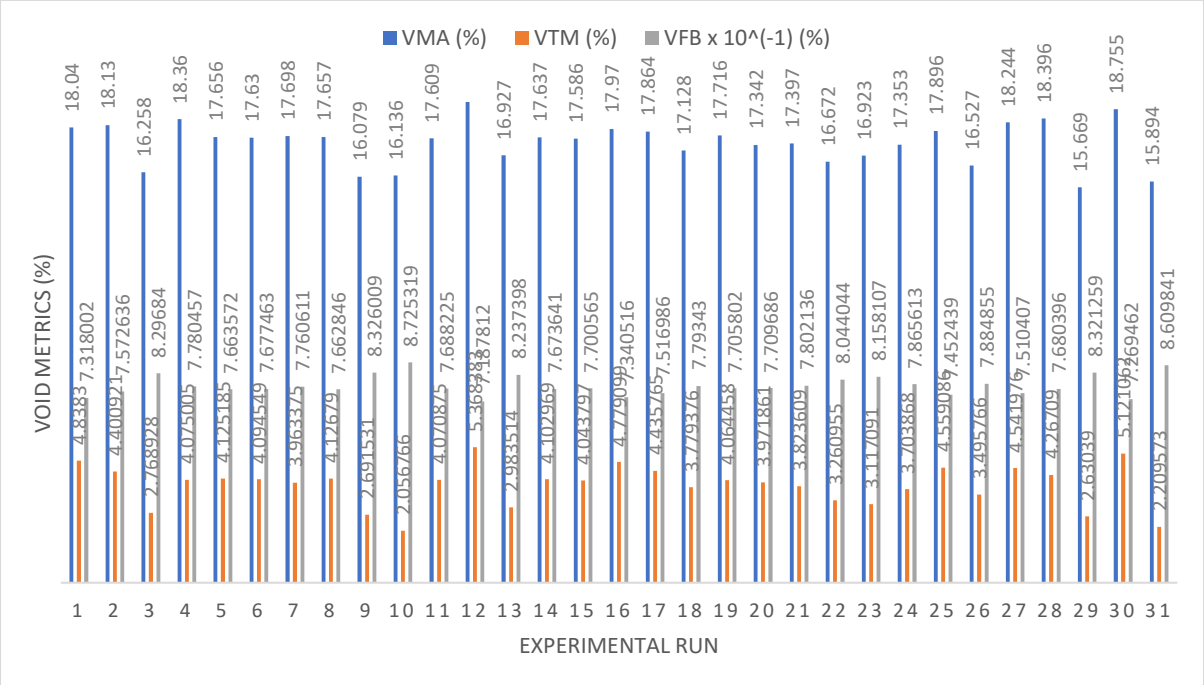

Figure 1. Void Properties of MK-DGAC

1.2 Response Surface Models (RSM) for Predicting the Volumetric Properties of MK-DGAC

3.2.1 RSM for Predicting VMA of MK-DGAC

Table 3 presents the matrix of the shape function and the experimentally determined VMA of MK- DGAC. On application of Equation (18), matrix D was obtained as given by Equation (21).

$$D = [540.24, 31063.2, 18630.46, 3457.66, 951.67, 1786182, 643511.7, 22133, 2706.67, 1071229, 198812, 54719.97, 119240, 32828.51, 6091.46\ ]^T \quad (21)$$

[E], being a 15 * 15 matrix was also obtained on application of Equation (19). With the help of [D] and [E], and application of Equation (20), the coefficient matrix of the VMA optimization model for predicting the VMA of MK-DGAC is obtained as presented by Equation (22).

$$\beta = [3697.15 \quad -119.224 \quad 23.173 \quad -200.293 \quad -8.672 \quad 1.263 \quad -0.150 \quad 22.704 \quad -0.030 \quad -0.344 \quad -2.224 \quad -0.003 \quad 1.057 \quad 0.057 \quad 1.017]^T \quad (22)$$

On substituting these coefficient values into Equation (11), the RSM optimization model for predicting the VMA of MK-DGAC was obtained as presented in Equation (23).

$$VMA = 3697.15 - 119.224Z_1 + 23.173\,Z_2 - 200.293Z_3 - 8.672Z_4 + 1.263\,Z_1^2 - 0.150\,Z_2^2 + 22.704\,Z_3^2 - 0.030\,Z_4^2 - 0.344\,Z_1Z_2 - 2.224\,Z_1Z_3 - 0.003\,Z_1Z_4 + 1.057\,Z_2Z_3 + 0.057\,Z_2Z_4 + 1.017\,Z_3Z_4 \quad (23)$$

Equation (23) introduces an optimization model designed to predict the VMA of MK-DGAC. The model's performance is evaluated using the coefficient of determination (R^2), which quantifies how well the model's predictions align with actual observed values. An R^2 value of 88.98% at a 5% significance level, as depicted in Figure 2, indicates that the model explains approximately 89% of the variability in VMA, signifying a strong predictive capability.

In regression analysis, an R^2 value approaching 1 suggests a model with high explanatory power. The obtained R^2 of 0.8898 implies that the model captures a substantial portion of the variance in VMA, leaving only about 11% unexplained. This level of accuracy is considered robust in engineering applications, where models with R^2 values above 0.85 are typically deemed reliable for predictive purposes.The statistical significance of the model at the 5% level further reinforces its validity. This means there's a less than 5% probability that the observed relationship between the predictors and VMA is due to random chance, underscoring the model's reliability.

The model's performance aligns with findings from recent studies in related fields. For instance, in the context of air quality prediction, a study reported R^2 values of 0.898 for Visakhapatnam and 0.9024 for Hyderabad, indicating strong model fits (Srinivas et al., 2024). Similarly, in the optimization of gas turbine power plants, R^2 values of 0.972 and 0.987 were achieved for specific fuel consumption and thermal efficiency, respectively, demonstrating high model accuracy (Akinlabi et al., 2025). The high R^2 value of the MK-DGAC model suggests that it can serve as a reliable tool for predicting VMA, which is crucial for assessing the durability and performance of asphalt mixtures. Accurate VMA predictions enable engineers to optimize mix designs, ensuring that the asphalt concrete meets desired specifications and performance criteria.

Table 3. Matrix of shape function [Z^n], and the VMA of MK-DGAC

Intercept	Z_1	Z_2	Z_3	Z_4	Z_1^2	Z_2^2	Z_3^2	Z_4^2	Z_1Z_2	Z_1Z_3	Z_1Z_4	Z_2Z_3	Z_2Z_4	Z_3Z_4	VMA
1	57	36.31	6.5	3.63	3249	1318.42	42.25	13.18	2069.67	370.50	206.91	236.02	131.81	23.60	18.040
1	57.5	34.495	6.4	0	3306.25	1189.91	40.96	0.00	1983.46	368.00	0.00	220.77	0.00	0.00	18.130
1	57.5	34.495	6.4	3.63	3306.25	1189.91	40.96	13.18	1983.46	368.00	208.73	220.77	125.22	23.23	16.258
1	57	32.68	6.5	0	3249	1067.98	42.25	0.00	1862.76	370.50	0.00	212.42	0.00	0.00	18.360
1	57.5	34.495	6.4	1.815	3306.25	1189.91	40.96	3.29	1983.46	368.00	104.36	220.77	62.61	11.62	17.656
1	57.5	34.495	6.4	1.815	3306.25	1189.91	40.96	3.29	1983.46	368.00	104.36	220.77	62.61	11.62	17.630
1	57.5	34.495	6.5	1.815	3306.25	1189.91	42.25	3.29	1983.46	373.75	104.36	224.22	62.61	11.80	17.698
1	57.5	34.495	6.4	1.815	3306.25	1189.91	40.96	3.29	1983.46	368.00	104.36	220.77	62.61	11.62	17.657
1	58	36.31	6.5	3.63	3364	1318.42	42.25	13.18	2105.98	377.00	210.54	236.02	131.81	23.60	16.079
1	57	32.68	6.5	3.63	3249	1067.98	42.25	13.18	1862.76	370.50	206.91	212.42	118.63	23.60	16.136
1	57.5	34.495	6.4	1.815	3306.25	1189.91	40.96	3.29	1983.46	368.00	104.36	220.77	62.61	11.62	17.609
1	57	32.68	6.3	0	3249	1067.98	39.69	0.00	1862.76	359.10	0.00	205.88	0.00	0.00	19.090
1	57.5	32.68	6.4	1.815	3306.25	1067.98	40.96	3.29	1879.10	368.00	104.36	209.15	59.31	11.62	16.927
1	57.5	34.495	6.4	1.815	3306.25	1189.91	40.96	3.29	1983.46	368.00	104.36	220.77	62.61	11.62	17.637
1	57.5	34.495	6.4	1.815	3306.25	1189.91	40.96	3.29	1983.46	368.00	104.36	220.77	62.61	11.62	17.586
1	58	36.31	6.3	0	3364	1318.42	39.69	0.00	2105.98	365.40	0.00	228.75	0.00	0.00	17.970
1	58	34.495	6.4	1.815	3364	1189.91	40.96	3.29	2000.71	371.20	105.27	220.77	62.61	11.62	17.864
1	58	32.68	6.3	3.63	3364	1067.98	39.69	13.18	1895.44	365.40	210.54	205.88	118.63	22.87	17.128
1	58	36.31	6.5	0	3364	1318.42	42.25	0.00	2105.98	377.00	0.00	236.02	0.00	0.00	17.716
1	57.5	34.495	6.3	1.815	3306.25	1189.91	39.69	3.29	1983.46	362.25	104.36	217.32	62.61	11.43	17.342
1	57.5	34.495	6.4	1.815	3306.25	1189.91	40.96	3.29	1983.46	368.00	104.36	220.77	62.61	11.62	17.397
1	57.5	36.31	6.4	1.815	3306.25	1318.42	40.96	3.29	2087.83	368.00	104.36	232.38	65.90	11.62	16.672
1	58	32.68	6.5	3.63	3364	1067.98	42.25	13.18	1895.44	377.00	210.54	212.42	118.63	23.60	16.923
1	57	34.495	6.4	1.815	3249	1189.91	40.96	3.29	1966.22	364.80	103.46	220.77	62.61	11.62	17.353

1	57	36.31	6.3	0	3249	1318.42	39.69	0.00	2069.67	359.10	0.00	228.75	0.00	0.00	17.896
1	57	36.31	6.3	3.63	3249	1318.42	39.69	13.18	2069.67	359.10	206.91	228.75	131.81	22.87	16.527
1	57	36.31	6.5	0	3249	1318.42	42.25	0.00	2069.67	370.50	0.00	236.02	0.00	0.00	18.244
1	58	32.68	6.5	0	3364	1067.98	42.25	0.00	1895.44	377.00	0.00	212.42	0.00	0.00	18.396
1	58	36.31	6.3	3.63	3364	1318.42	39.69	13.18	2105.98	365.40	210.54	228.75	131.81	22.87	15.669
1	58	32.68	6.3	0	3364	1067.98	39.69	0.00	1895.44	365.40	0.00	205.88	0.00	0.00	18.755
1	57	32.68	6.3	3.63	3249	1067.98	39.69	13.18	1862.76	359.10	206.91	205.88	118.63	22.87	15.894

Z_1= granite proportion; Z_2 = granular sand proportion; Z_3 = bitumen proportion.; Z_4 = MK proportion

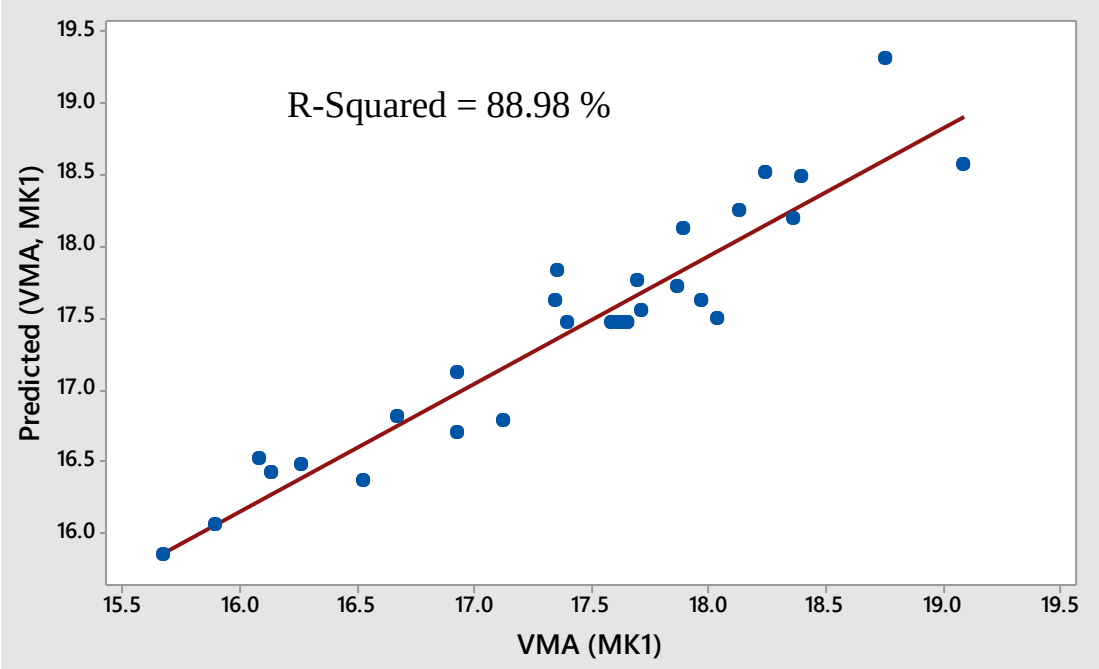

Figure 2. R^2Statistics of Developed VMA of MK-DGAC

3.2.2 RSM for Predicting VTM of MK-DGAC

Table 4 presents the matrix of the shape function and the experimentally determined VTM of the MK- DGAC. On application of Equation (18), D for VTM of MK-DGAC was obtained as given by Equation (24).

$$D = [119.47, 6869.65, 4124.60, 764.39, 192.18, 395023.6, 142619.6, 4891.32, 530.56, 237160, 43952.46, 11050.14, 26390.19, 6646.48, 1230.14\ ]^T \quad (24)$$

[E], being a 15 * 15 matrix was also obtained on application of Equation (20). With the help of [D] and [E], and application of Equation (19), the coefficient matrix of the VTM optimization model for MK-DGAC is obtained as presented by Equation (25).

$$\beta = [4291.534\ \ -138.525\ \ 27.236\ \ -238.274\ \ -9.866\ \ 1.468\ \ -0.176\ \ 26.479\ \ -0.036\ \ -0.403\ \ -2.561\ \ -0.005\ \ 1.252\ \ 0.064\ \ 1.194]^T \quad (25)$$

On substituting these coefficient values into Equation (11), the RSM optimization model for predicting the VTM of MK -DGAC was obtained as presented in Equation (26).

$$VTM = 4291.534 - 138.525Z_1 + 27.236\,Z_2 - 238.274Z_3 - 9.866Z_4 + 1.468\,Z_1^2 - 0.176\,Z_2^2 + 26.479\,Z_3^2 - 0.036\,Z_4^2 - 0.403\,Z_1Z_2 - 2.561\,Z_1Z_3 - 0.005\,Z_1Z_4 + 1.252\,Z_2Z_3 + 0.064\,Z_2Z_4 + 1.194\,Z_3Z_4 \quad (26)$$

Equation (26) introduces an optimization model aimed at predicting and optimizing the VTM of MK-DGAC. The model's performance is evaluated using the coefficient of determination (R^2), which quantifies how well the model's predictions align with actual observed values. An R^2 value of 83.96% (Figure 3) at a 5% significance level indicates that the model explains approximately 84% of the variability in VTM, signifying a strong predictive capability.

In the context of regression modeling, an R^2 value greater than 0.75 is generally accepted as indicative of a good model fit in engineering and materials science applications. The R^2 value of 0.8396 obtained here suggests that the model is robust, explaining nearly 84% of the variability in VTM. This demonstrates that the mix design parameters incorporated in the model are strong predictors of VTM. Furthermore, the model's statistical significance at the 5% level means that there is less than a 5% chance that the observed relationship is due to random variation, reinforcing the reliability of the model (Srinivas et al., 2024).

While a high R^2 value supports the model's explanatory power, it is essential to interpret this metric alongside other model validation indicators, such as Root Mean Square Error (RMSE) and Mean Absolute Error (MAE), particularly in multivariate models (Siegel, 2012). This approach helps ensure that the model is both accurate and generalizable. The 83.96% R^2 indicates that the model's predictive strength is sufficiently robust for practical use in asphalt mix optimization.

VTM is a critical quality parameter that influences key performance properties such as air void content, moisture resistance, and long-term durability of asphalt concrete. Accurate prediction of VTM allows engineers to design mixtures that optimize these properties while maintaining structural integrity and cost-efficiency. A model with an R^2 of 83.96% provides practitioners with a dependable tool for assessing and adjusting MK-DGAC mix designs (Siegel, 2012).

Table 4. Matrix of shape function [Z^n], and the VTM of MK-DGAC

Intercept	Z_1	Z_2	Z_3	Z_4	Z_1^2	Z_2^2	Z_3^2	Z_4^2	Z_1Z_2	Z_1Z_3	Z_1Z_4	Z_2Z_3	Z_2Z_4	Z_3Z_4	VTM
1	57	36.31	6.5	3.63	3249	1318.42	42.25	13.18	2069.67	370.50	206.91	236.02	131.81	23.60	4.838
1	57.5	34.495	6.4	0	3306.25	1189.91	40.96	0.00	1983.46	368.00	0.00	220.77	0.00	0.00	4.401
1	57.5	34.495	6.4	3.63	3306.25	1189.91	40.96	13.18	1983.46	368.00	208.73	220.77	125.22	23.23	2.769
1	57	32.68	6.5	0	3249	1067.98	42.25	0.00	1862.76	370.50	0.00	212.42	0.00	0.00	4.075
1	57.5	34.495	6.4	1.815	3306.25	1189.91	40.96	3.29	1983.46	368.00	104.36	220.77	62.61	11.62	4.125
1	57.5	34.495	6.4	1.815	3306.25	1189.91	40.96	3.29	1983.46	368.00	104.36	220.77	62.61	11.62	4.095
1	57.5	34.495	6.5	1.815	3306.25	1189.91	42.25	3.29	1983.46	373.75	104.36	224.22	62.61	11.80	3.963
1	57.5	34.495	6.4	1.815	3306.25	1189.91	40.96	3.29	1983.46	368.00	104.36	220.77	62.61	11.62	4.127
1	58	36.31	6.5	3.63	3364	1318.42	42.25	13.18	2105.98	377.00	210.54	236.02	131.81	23.60	2.692
1	57	32.68	6.5	3.63	3249	1067.98	42.25	13.18	1862.76	370.50	206.91	212.42	118.63	23.60	2.057
1	57.5	34.495	6.4	1.815	3306.25	1189.91	40.96	3.29	1983.46	368.00	104.36	220.77	62.61	11.62	4.071
1	57	32.68	6.3	0	3249	1067.98	39.69	0.00	1862.76	359.10	0.00	205.88	0.00	0.00	5.368
1	57.5	32.68	6.4	1.815	3306.25	1067.98	40.96	3.29	1879.10	368.00	104.36	209.15	59.31	11.62	2.984
1	57.5	34.495	6.4	1.815	3306.25	1189.91	40.96	3.29	1983.46	368.00	104.36	220.77	62.61	11.62	4.103
1	57.5	34.495	6.4	1.815	3306.25	1189.91	40.96	3.29	1983.46	368.00	104.36	220.77	62.61	11.62	4.044
1	58	36.31	6.3	0	3364	1318.42	39.69	0.00	2105.98	365.40	0.00	228.75	0.00	0.00	4.779
1	58	34.495	6.4	1.815	3364	1189.91	40.96	3.29	2000.71	371.20	105.27	220.77	62.61	11.62	4.436
1	58	32.68	6.3	3.63	3364	1067.98	39.69	13.18	1895.44	365.40	210.54	205.88	118.63	22.87	3.779
1	58	36.31	6.5	0	3364	1318.42	42.25	0.00	2105.98	377.00	0.00	236.02	0.00	0.00	4.064
1	57.5	34.495	6.3	1.815	3306.25	1189.91	39.69	3.29	1983.46	362.25	104.36	217.32	62.61	11.43	3.972
1	57.5	34.495	6.4	1.815	3306.25	1189.91	40.96	3.29	1983.46	368.00	104.36	220.77	62.61	11.62	3.824
1	57.5	36.31	6.4	1.815	3306.25	1318.42	40.96	3.29	2087.83	368.00	104.36	232.38	65.90	11.62	3.261
1	58	32.68	6.5	3.63	3364	1067.98	42.25	13.18	1895.44	377.00	210.54	212.42	118.63	23.60	3.117
1	57	34.495	6.4	1.815	3249	1189.91	40.96	3.29	1966.22	364.80	103.46	220.77	62.61	11.62	3.704
1	57	36.31	6.3	0	3249	1318.42	39.69	0.00	2069.67	359.10	0.00	228.75	0.00	0.00	4.559
1	57	36.31	6.3	3.63	3249	1318.42	39.69	13.18	2069.67	359.10	206.91	228.75	131.81	22.87	3.496
1	57	36.31	6.5	0	3249	1318.42	42.25	0.00	2069.67	370.50	0.00	236.02	0.00	0.00	4.542
1	58	32.68	6.5	0	3364	1067.98	42.25	0.00	1895.44	377.00	0.00	212.42	0.00	0.00	4.267
1	58	36.31	6.3	3.63	3364	1318.42	39.69	13.18	2105.98	365.40	210.54	228.75	131.81	22.87	2.630
1	58	32.68	6.3	0	3364	1067.98	39.69	0.00	1895.44	365.40	0.00	205.88	0.00	0.00	5.121
1	57	32.68	6.3	3.63	3249	1067.98	39.69	13.18	1862.76	359.10	206.91	205.88	118.63	22.87	2.210

Z_1= granite proportion; Z_2 = granular sand proportion; Z_3 = bitumen proportion.; Z_4 = MK proportion

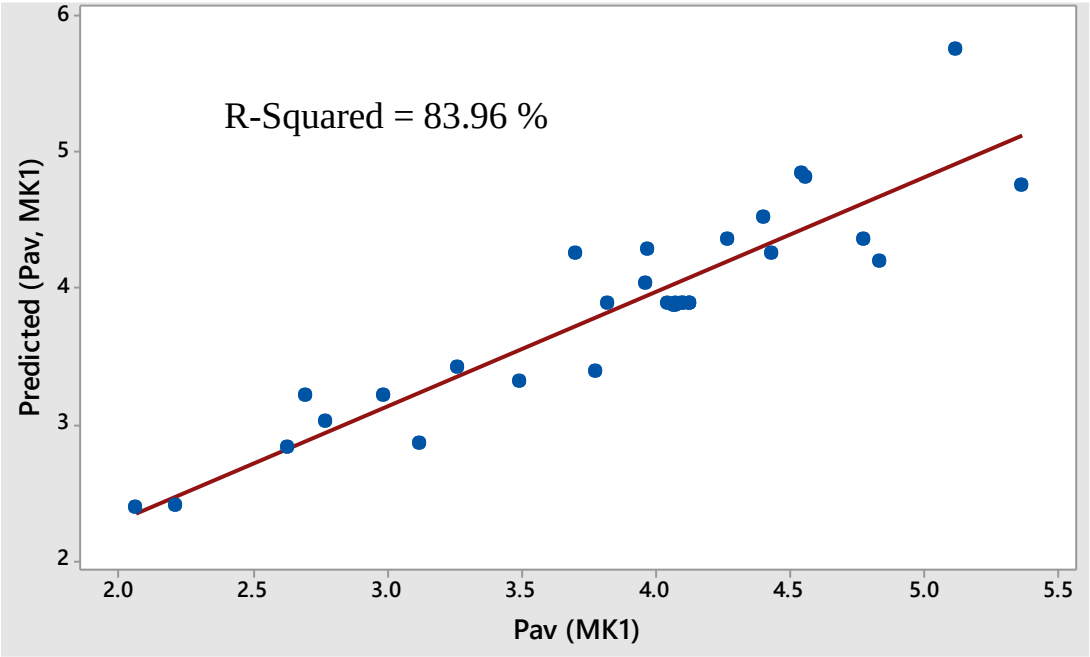

Figure 3. R^2 statistics of Developed VTM of MK-DGAC

3.2.3 RSM for Predicting VFB of MK-DGAC

Table 5 presents the matrix of the shape function and the experimentally determined VFB of MK- DGAC. On application of Equation (18), D for VFB of MK-DGAC was obtained as given by Equation (27).

$$D = [2419.36, 139112.3, 83428.02, 15485.32, 4498.842, 7999244, 2881542, 99129.06, 13003.54, 4797099, 890399.5, 258681.4, 533984.5, \ 155086.6, 28792.39\ ]^T \quad (27)$$

Matrix [E], being a 15 * 15 matrix was also obtained on application of Equation (20). With the help of [D] and [E], and application of Equation (19), the coefficient matrix of the VFB optimization model for MK-DGAC is obtained as presented by Equation (28).

$$\beta = [-19592.896 \ \ 637.793 \ \ -138.669 \ \ 1148.192 \ \ 44.428 \ \ -6.811 \ 0.847 \ \ -126.445 \ \ 0.222 \ \ 2.018 \ \ 11.830 \ \ -0.003 \ \ -5.587 \ \ -0.290 \ \ -5.196]^T \quad (28)$$

On substituting these coefficient values into Equation (11), the RSM optimization model for predicting the VFB of MK-DGAC was obtained as presented in Equation (29).

$$VFB = -19592.896 + 637.739Z_1 - 138.669\,Z_2 + 1148.192Z_3 + 44.428Z_4 - 6.811\,Z_1^2 + 0.847\,Z_2^2 - 126.445\,Z_3^2 + 0.222\,Z_4^2 + 2.018\,Z_1Z_2 + 11.830\,Z_1Z_3 - 0.003\,Z_1Z_4 - 5.587\,Z_2Z_3 - 0.290\,Z_2Z_4 - 5.196\,Z_3Z_4 \quad (29)$$

Equation (29) in the present study represents the optimization model formulated to predict and optimize the VFB in MK-DGAC. The model integrates key input parameters such as metakaolin dosage, aggregate gradation, and binder content to accurately forecast the VFB, which directly influences durability and moisture resistance. The application of Response Surface Methodology (RSM) likely underpins this model, a widely accepted technique for developing predictive equations in civil engineering materials (Usman & Uthman, 2020).

The performance of the model is supported by a coefficient of determination (R^2) of 82.62% (Figure 4), calculated at a 5% level of significance. This implies that the model accounts for approximately 82.62% of the variation in the VFB, indicating substantial predictive accuracy. In materials science and pavement engineering, R^2 values above 80% are generally considered robust for practical applications (Wikipedia, 2025).

Comparative studies validate the adequacy of this R^2 value. For example, Usman and Uthman (2020) demonstrated similar statistical strength in biodiesel optimization models, reporting R^2 values exceeding 85%. In the context of cementitious materials, a study by Olofinnade et al. (2023) using RSM to predict the performance of concrete containing ground scoria and metakaolin achieved R^2 values of 79.44% for water absorption and over 90% for density and compressive strength. These findings align with the current study's outcome, reinforcing the claim that the model in Equation (29) is statistically sound and practically applicable.

Moreover, the use of RSM facilitates both prediction and optimization, a dual capability critical for fine-tuning MK-DGAC formulations under varying field conditions. As emphasized by Saha (2023), models that integrate optimization tools provide a systematic approach to enhancing process efficiency, especially where multiple interacting variables exist.

Thus, the R^2 value of 82.62% confirms that the optimization model represented by Equation (29) is suitable for engineering predictions, ensuring reliability in forecasting the VFB in MK-DGAC. The model provides a strategic tool for mix design engineers seeking to balance performance requirements and sustainability goals in modern pavement materials.

Table 5. Matrix of shape function [Z^n], and the VFB of MK-DGAC

Intercept	Z_1	Z_2	Z_3	Z_4	Z_1^2	Z_2^2	Z_3^2	Z_4^2	Z_1Z_2	Z_1Z_3	Z_1Z_4	Z_2Z_3	Z_2Z_4	Z_3Z_4	VFB
1	57	36.31	6.5	3.63	3249	1318.42	42.25	13.18	2069.67	370.50	206.91	236.02	131.81	23.60	73.18
1	57.5	34.495	6.4	0	3306.25	1189.91	40.96	0.00	1983.46	368.00	0.00	220.77	0.00	0.00	75.73
1	57.5	34.495	6.4	3.63	3306.25	1189.91	40.96	13.18	1983.46	368.00	208.73	220.77	125.22	23.23	82.97
1	57	32.68	6.5	0	3249	1067.98	42.25	0.00	1862.76	370.50	0.00	212.42	0.00	0.00	77.80
1	57.5	34.495	6.4	1.815	3306.25	1189.91	40.96	3.29	1983.46	368.00	104.36	220.77	62.61	11.62	76.64
1	57.5	34.495	6.4	1.815	3306.25	1189.91	40.96	3.29	1983.46	368.00	104.36	220.77	62.61	11.62	76.77
1	57.5	34.495	6.5	1.815	3306.25	1189.91	42.25	3.29	1983.46	373.75	104.36	224.22	62.61	11.80	77.61
1	57.5	34.495	6.4	1.815	3306.25	1189.91	40.96	3.29	1983.46	368.00	104.36	220.77	62.61	11.62	76.63
1	58	36.31	6.5	3.63	3364	1318.42	42.25	13.18	2105.98	377.00	210.54	236.02	131.81	23.60	83.26
1	57	32.68	6.5	3.63	3249	1067.98	42.25	13.18	1862.76	370.50	206.91	212.42	118.63	23.60	87.25
1	57.5	34.495	6.4	1.815	3306.25	1189.91	40.96	3.29	1983.46	368.00	104.36	220.77	62.61	11.62	76.88
1	57	32.68	6.3	0	3249	1067.98	39.69	0.00	1862.76	359.10	0.00	205.88	0.00	0.00	71.88
1	57.5	32.68	6.4	1.815	3306.25	1067.98	40.96	3.29	1879.10	368.00	104.36	209.15	59.31	11.62	82.37
1	57.5	34.495	6.4	1.815	3306.25	1189.91	40.96	3.29	1983.46	368.00	104.36	220.77	62.61	11.62	76.74
1	57.5	34.495	6.4	1.815	3306.25	1189.91	40.96	3.29	1983.46	368.00	104.36	220.77	62.61	11.62	77.01
1	58	36.31	6.3	0	3364	1318.42	39.69	0.00	2105.98	365.40	0.00	228.75	0.00	0.00	73.41
1	58	34.495	6.4	1.815	3364	1189.91	40.96	3.29	2000.71	371.20	105.27	220.77	62.61	11.62	75.17
1	58	32.68	6.3	3.63	3364	1067.98	39.69	13.18	1895.44	365.40	210.54	205.88	118.63	22.87	77.93
1	58	36.31	6.5	0	3364	1318.42	42.25	0.00	2105.98	377.00	0.00	236.02	0.00	0.00	77.06
1	57.5	34.495	6.3	1.815	3306.25	1189.91	39.69	3.29	1983.46	362.25	104.36	217.32	62.61	11.43	77.10
1	57.5	34.495	6.4	1.815	3306.25	1189.91	40.96	3.29	1983.46	368.00	104.36	220.77	62.61	11.62	78.02
1	57.5	36.31	6.4	1.815	3306.25	1318.42	40.96	3.29	2087.83	368.00	104.36	232.38	65.90	11.62	80.44
1	58	32.68	6.5	3.63	3364	1067.98	42.25	13.18	1895.44	377.00	210.54	212.42	118.63	23.60	81.58
1	57	34.495	6.4	1.815	3249	1189.91	40.96	3.29	1966.22	364.80	103.46	220.77	62.61	11.62	78.66
1	57	36.31	6.3	0	3249	1318.42	39.69	0.00	2069.67	359.10	0.00	228.75	0.00	0.00	74.52
1	57	36.31	6.3	3.63	3249	1318.42	39.69	13.18	2069.67	359.10	206.91	228.75	131.81	22.87	78.85
1	57	36.31	6.5	0	3249	1318.42	42.25	0.00	2069.67	370.50	0.00	236.02	0.00	0.00	75.10
1	58	32.68	6.5	0	3364	1067.98	42.25	0.00	1895.44	377.00	0.00	212.42	0.00	0.00	76.80
1	58	36.31	6.3	3.63	3364	1318.42	39.69	13.18	2105.98	365.40	210.54	228.75	131.81	22.87	83.21
1	58	32.68	6.3	0	3364	1067.98	39.69	0.00	1895.44	365.40	0.00	205.88	0.00	0.00	72.69
1	57	32.68	6.3	3.63	3249	1067.98	39.69	13.18	1862.76	359.10	206.91	205.88	118.63	22.87	86.10

Z_1= granite proportion; Z_2 = sand proportion; Z_3 = bitumen proportion.; Z_4 = MK proportion

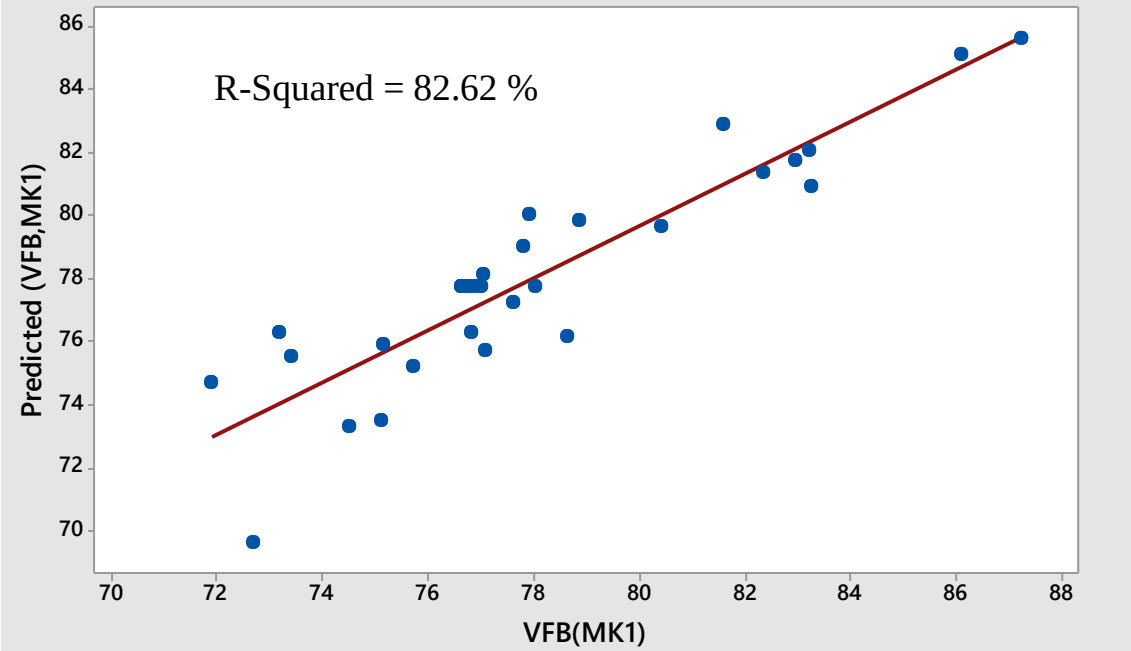

Figure 4. R^2 statistics of Developed VFB of MK-DGAC

3.3 Effect of Constituents on the Void Properties of MK-DGAC

3.3.1 Effect of Constituents on the VMA of MK-DGAC

Figure 5 illustrates the main effect plots used to evaluate the individual impact of constituents on the Voids in Mineral Aggregate (VMA) of Metakaolin-Densely Graded Asphalt Concrete (MK-DGAC). The steepness of each plot reflects the magnitude of influence a constituent exerts on the VMA. A horizontal line indicates minimal effect, while a steep slope signifies a strong influence. Among the constituents, metakaolin (MK) demonstrated the most significant effect, as evidenced by its steep curve. As MK content increased from 0% to 3.63%, the mean VMA decreased linearly from 18.25% to approximately 16.5%, which corresponds to a percentage reduction of around 9.6%. This decrease in VMA with increasing MK is attributed to the pozzolanic nature and fine particle size of MK, which tends to occupy voids within the aggregate skeleton and densify the mix, leading to lower VMA. A similar trend has been reported by Ali et al. (2012), who found that mineral fillers like MK reduce void content by enhancing the compactness of asphalt mixtures.

Sand exhibited the second most pronounced effect on VMA. The VMA increased from 17.1% at 32.68% sand content to 17.5% at 34.495% sand, marking a 2.34% rise. However, a further increase in sand to 36.31% caused the VMA to decline to 16.7%, representing a 4.57% reduction. The initial increase in VMA is likely due to improved packing and grain interlocking, while the subsequent decrease may be due to oversaturation, where excess sand leads to a denser configuration that reduces void spaces. This behavior aligns with the findings of Rahman et al. (2012), who reported that optimal sand levels improve VMA, but excessive amounts could lead to tighter compaction and decreased voids.

Bitumen's effect on VMA was more moderate. As the bitumen content increased from 6.3% to 6.4%, the mean VMA dropped from 17.6% to 17.5%, a reduction of 0.6%. However, increasing the bitumen content to 6.5% reversed this trend, raising the VMA to 17.75%, which represents a 1.43% increase. This behavior suggests that at lower bitumen levels, improved lubrication facilitates better aggregate packing, hence reducing VMA, while at higher contents, the excess bitumen acts as a cushion between particles, increasing the overall VMA. Pourtahmasb et al. (2014) observed similar nonlinear behavior in asphalt mixes, where bitumen content initially reduced voids but began to increase them at higher dosages due to lubrication effects.

Granite had the least impact on VMA. A slight decrease in VMA from 17.80% to 17.49% occurred as granite content increased from 57.00% to 57.5%, amounting to a 1.71% reduction. Beyond this, as granite content reached 58.0%, the VMA slightly rose to 17.70%, a 1.20% increase. These marginal variations suggest that granite's influence on VMA is minimal, likely because its coarse gradation and inert behavior do not significantly alter the internal structure of the mix. Rahman et al. (2012) similarly noted that coarser aggregates like granite have less influence on VMA compared to finer constituents.

The analysis is supported by ANOVA results, where the significance of each constituent's effect was statistically verified. At a 5% level of significance, MK had the smallest p-value of 0.000, confirming its dominant influence on VMA. This was followed by sand ($p = 0.104$), indicating a notable, though not statistically significant, effect. Granite and bitumen, with p-values of 0.531 and 0.428 respectively, had the least statistically significant

impacts on VMA. These findings highlight that while all constituents contribute to the behavior of MK-DGAC, MK and sand play the most critical roles in influencing VMA.

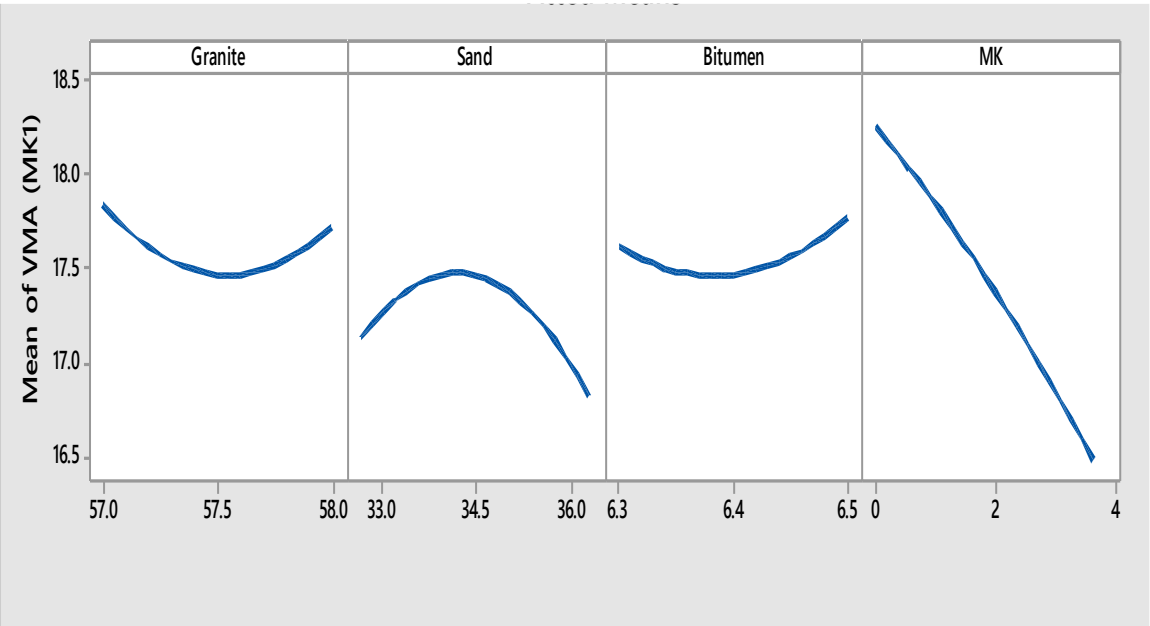

Figure 5. Main Effects Plots for VMA of MK-DGAC

Table 6ANOVA Statistics for Effect Analysis of Constituents of Mk-DGAC on VMA

Source	DF	Adj SS	Adj MS	F-Value	P-Value
Model	14	18.9225	1.3516	9.23	0.000
Linear	4	14.6416	3.6604	24.98	0.000
Granite	1	0.0601	0.0601	0.41	0.531
Sand	1	0.4341	0.4341	2.96	0.104
Bitumen	1	0.0969	0.0969	0.66	0.428
MK	1	14.0506	14.0506	95.90	0.000
Square	4	0.8239	0.2060	1.41	0.277
Granite*Granite	1	0.2586	0.2586	1.77	0.203
Sand*Sand	1	0.6329	0.6329	4.32	0.054
Bitumen*Bitumen	1	0.1338	0.1338	0.91	0.354
MK*MK	1	0.0255	0.0255	0.17	0.682
2-Way Interaction	6	3.4570	0.5762	3.93	0.013
Granite*Sand	1	1.5598	1.5598	10.65	0.005
Granite*Bitumen	1	0.1979	0.1979	1.35	0.262
Granite*MK	1	0.0001	0.0001	0.00	0.976
Sand*Bitumen	1	0.5886	0.5886	4.02	0.062
Sand*MK	1	0.5653	0.5653	3.86	0.067
Bitumen*MK	1	0.5453	0.5453	3.72	0.072
Error	16	2.3442	0.1465		
Lack-of-Fit	10	2.2941	0.2294	27.50	0.000
Pure Error	6	0.0501	0.0083		
Total	30	21.2667			

3.3.2 Effect of Constituents on the VTM of MK-DGAC

The main effect plots in Figure 6 provide a visual representation of how various constituents influence the mean VTM of MK-DGAC. A steeper slope in these plots indicates a more significant impact on VTM, while a flatter slope suggests a lesser effect.

Metakaolin (MK) exhibits the most pronounced effect on VTM. As the MK content increases from 0% to 3.63%, the mean VTM decreases from 4.5% to approximately 3.0%, representing a 33.33% reduction. This trend is corroborated by the Analysis of Variance (ANOVA) results in Table 7, where MK has a P-value of 0.000, indicating a statistically significant impact on VTM. The reduction in VTM with increasing MK content can be attributed to the fine particle size and pozzolanic activity of MK, which enhance the packing density and

reduce air voids in the mix. This observation aligns with findings by Murana et al. (2014), who reported that incorporating MK as a partial replacement for cement in hot mix asphalt improves the mixture's density and reduces voids.

Bitumen content is the second most influential factor affecting VTM. An increase in bitumen content from 6.3% to 6.4% leads to a decrease in mean VTM from 4.30% to 3.70%, a 13.95% reduction. However, further increasing the bitumen content to 6.5% results in a slight increase in VTM to 3.85%, a 4.05% rise. The initial decrease in VTM can be attributed to improved coating and lubrication of aggregates, enhancing compaction. The subsequent increase may be due to excess bitumen creating a film that prevents proper aggregate interlock, leading to higher voids. The ANOVA results support this, with bitumen showing a P-value of 0.241, indicating a moderate impact on VTM. This behavior is consistent with the study by Ali et al. (2012), which found that increasing bitumen content initially reduces VTM, but excessive bitumen can lead to higher voids due to over-lubrication.

Sand content also plays a significant role in influencing VTM. As sand content increases from 32.68% to 34.495%, the mean VTM rises from 3.25% to 3.80%, a 16.90% increase. However, further increasing sand content to 36.31% results in a decrease in VTM to 3.50%, a 7.89% reduction. The initial increase in VTM may be due to the angularity and texture of sand particles, which can create more voids. The subsequent decrease could be attributed to improved packing and reduced voids at higher sand contents. The ANOVA results show a P-value of 0.333 for sand, indicating a moderate effect on VTM. This trend aligns with the findings of Islam et al. (2019), who observed that sand particle size and distribution significantly affect the void content in granular materials.

Granite, as the final constituent, has the least impact on VTM. An increase in granite content from 57.00% to 57.5% leads to a decrease in mean VTM from 4.25% to 3.90%, an 8.24% reduction. Further increasing granite content to 58.0% results in an increase in VTM back to 4.25%, an 8.24% rise. This symmetrical change suggests that granite content has a negligible net effect on VTM. The ANOVA results confirm this, with granite showing a P-value of 0.985, indicating an insignificant impact on VTM. This observation is supported by the study of Islam et al. (2019), which found that the particle size of sand influences the shear strength and void content of granular materials.

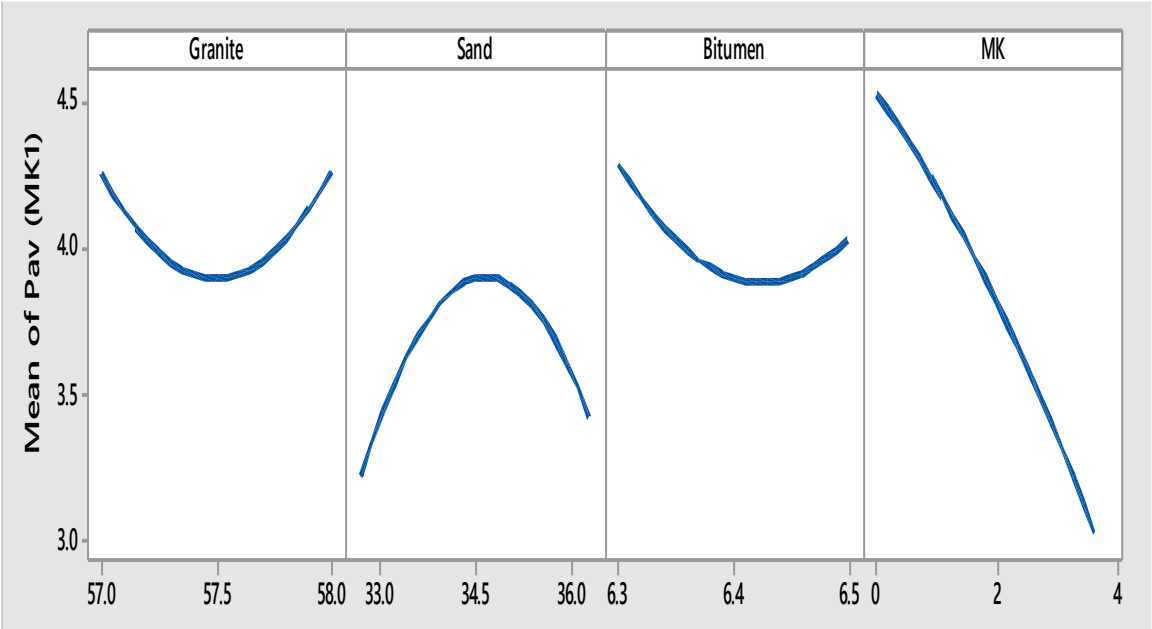

Figure 6. Main Effects Plots for VTM of MK -DGAC

Table 7; ANOVA Statistics for Effect Analysis of Constituents of MK-DGACon VTM

Source	DF	Adj SS	Adj MS	F-Value	P-Value
Model	14	16.5754	1.1840	5.98	0.001
Linear	4	10.7503	2.6876	13.58	0.000
Granite	1	0.0001	0.0001	0.00	0.985
Sand	1	0.1971	0.1971	1.00	0.333
Bitumen	1	0.2936	0.2936	1.48	0.241
MK	1	10.2595	10.2595	51.84	0.000
Square	4	1.1363	0.2841	1.44	0.268
Granite*Granite	1	0.3495	0.3495	1.77	0.203
Sand*Sand	1	0.8748	0.8748	4.42	0.052
Bitumen*Bitumen	1	0.1820	0.1820	0.92	0.352
MK*MK	1	0.0361	0.0361	0.18	0.675
2-Way Interaction	6	4.6888	0.7815	3.95	0.013
Granite*Sand	1	2.1349	2.1349	10.79	0.005
Granite*Bitumen	1	0.2624	0.2624	1.33	0.266
Granite*MK	1	0.0003	0.0003	0.00	0.969
Sand*Bitumen	1	0.8255	0.8255	4.17	0.058
Sand*MK	1	0.7141	0.7141	3.61	0.076
Bitumen*MK	1	0.7516	0.7516	3.80	0.069
Error	16	3.1666	0.1979		
Lack-of-Fit	10	3.0987	0.3099	27.40	0.000
Pure Error	6	0.0679	0.0113		
Total	30	19.7420			

3.3.3 Effect of Constituents on the VFB of MK-DGAC

The analysis of the main effect plots and ANOVA results reveals the influence of various constituents on the mean Voids Filled with Bitumen (VFB) in Metakaolin-Modified Dense Graded Asphalt Concrete (MK-DGAC). The steepness of the slope in the main effect plots indicates the magnitude of each constituent's impact on VFB.

Metakaolin (MK) exhibits the most significant effect on mean VFB. As the MK content increases from 0% to 3.63%, the mean VFB increases almost linearly from 75.00% to approximately 82.0%, representing a 9.33% increase. This substantial effect is corroborated by the ANOVA results, where MK has a P-value of 0.000, indicating a statistically significant impact on mean VFB at the 5% significance level. This finding aligns with previous studies that have demonstrated the positive impact of metakaolin on the volumetric properties of asphalt mixtures (Ragab, 2023).

Sand content shows a quadratic effect on mean VFB. Initially, as sand content increases from 32.68% to 34.495%, the mean VFB decreases from 81.5% to 78.0%, a 4.29% reduction. Beyond 34.495% sand content, the mean VFB increases to 79.50% at 36.31%, a 1.92% rise. Overall, the greater magnitude of decrease compared to the subsequent increase suggests that sand has an overall negative effect on mean VFB. The ANOVA results support this observation, with sand having a P-value of 0.111, ranking second in its impact on mean VFB. This trend is consistent with findings by Shuaibu et al. (2021), who reported that increasing silica sand content in asphalt mixtures leads to a decrease in VFB due to the sand particles absorbing effective bitumen.

Bitumen content also affects mean VFB, albeit to a lesser extent. An increase in bitumen content from 6.3% to 6.4% leads to an increase in mean VFB from 76.5% to 78.0%, a 1.96% rise. However, further increasing bitumen content to 6.5% results in a slight decrease in mean VFB to 77.5%, a 0.006% reduction. Since the increase is greater than the decrease, bitumen is considered to have a slight overall positive effect on mean VFB. This is reflected in the ANOVA results, where bitumen has a P-value of 0.146, ranking third in its impact on mean VFB. Similar observations were made by Ibedu and Murana (2024), who found that VFB generally increases with bitumen content up to a certain point, beyond which it may decrease due to over-saturation

Granite content exhibits the least impact on mean VFB. As granite content increases from 57.00% to 57.5%, the mean VFB increases from 76.25% to 78.0%, a 2.30% increment. However, further increasing granite content to 58.0% results in a decrease in mean VFB back to 76.25%, a 2.30% reduction. The equal magnitude of increase and decrease suggests that granite has no net effect on mean VFB. The ANOVA results confirm this, with granite having a P-value of 0.810, indicating no significant impact on mean VFB.

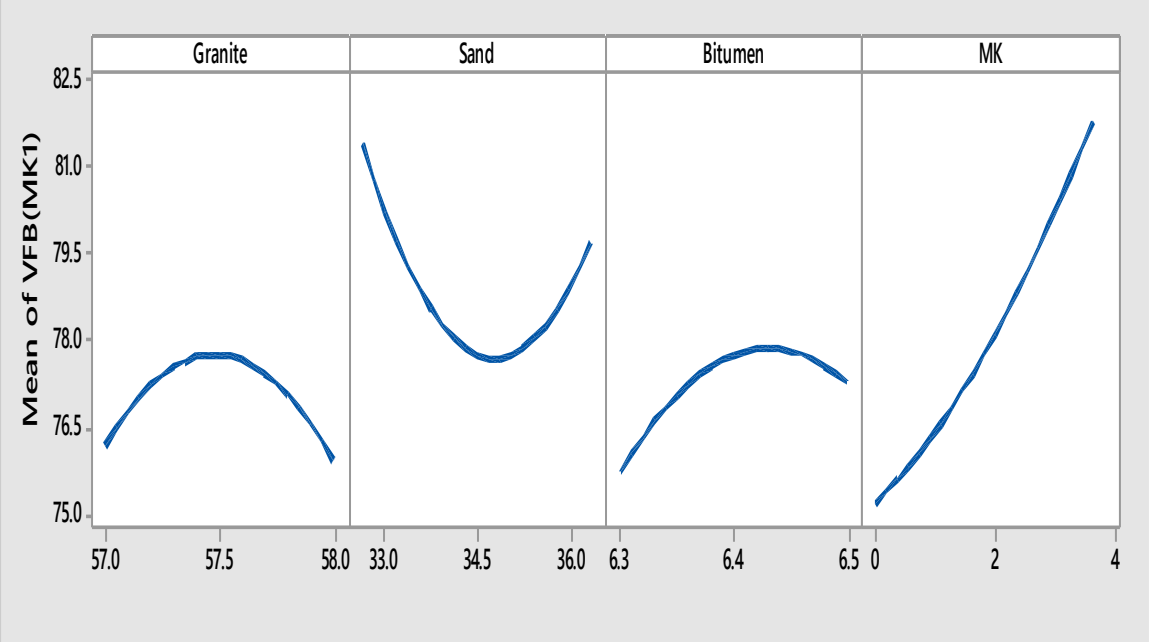

Figure 7. Main Effects Plots for VFB of MK -DGAC.

Table 8; ANOVA Statistics for Effect Analysis of Constituents of MK-DGAC on VFB

Source	DF	Adj SS	Adj MS	F-Value	P-Value
Model	14	351.742	25.124	5.43	0.001
Linear	4	219.863	54.966	11.88	0.000
Granite	1	0.276	0.276	0.06	0.810
Sand	1	13.157	13.157	2.84	0.111
Bitumen	1	10.824	10.824	2.34	0.146
MK	1	195.607	195.607	42.28	0.000
Square	4	27.361	6.840	1.48	0.255
Granite*Granite	1	7.526	7.526	1.63	0.220
Sand*Sand	1	20.219	20.219	4.37	0.053
Bitumen*Bitumen	1	4.149	4.149	0.90	0.358
MK*MK	1	1.388	1.388	0.30	0.591
2-Way Interaction	6	104.518	17.420	3.77	0.016
Granite*Sand	1	53.653	53.653	11.60	0.004
Granite*Bitumen	1	5.598	5.598	1.21	0.288
Granite*MK	1	0.000	0.000	0.00	0.996
Sand*Bitumen	1	16.455	16.455	3.56	0.078
Sand*MK	1	14.585	14.585	3.15	0.095
Bitumen*MK	1	14.228	14.228	3.08	0.099
Error	16	74.015	4.626		
Lack-of-Fit	10	72.581	7.258	30.37	0.000
Pure Error	6	1.434	0.239		
Total	30	425.757			

3.4 Multi-Objective Optimization of MK-DGAC for Maximum Performance

The optimization of metakaolin-densified graded asphalt concrete (MK-DGAC) mix design aims to enhance performance across key volumetric properties: voids in mineral aggregate (VMA), voids in total mix (VTM), and voids filled with bitumen (VFB). Figure 8 illustrates the optimal composition derived through response surface methodology (RSM), a statistical technique widely employed in asphalt mixture optimization (Fan et al., 2023). The ideal mix comprises 57.253% granite, 32.680% granular sand, 6.399% bitumen, and 3.63% MK. When normalized to a 100% scale, these proportions adjust slightly to 57.275% granite, 32.692% sand, 6.401% bitumen, and 3.631% MK.

The optimized formulation of MK-DGAC achieves a composite desirability score of 96.95%, indicating a highly effective balance among the volumetric properties critical for asphalt mixture performance. Specifically,

the mix attains a minimized VMA of 15.899%, a VTM of 2.034%, and a VFB of 86.897%, with desirability scores of 93.28%, 1.000, and 97.68%, respectively. These optimized values reflect a mix design that not only meets but, in several respects, exceeds established standards and specifications.

According to the Superpave volumetric mix design criteria, widely used across the pavement engineering field and formalized by the American Association of State Highway and Transportation Officials (AASHTO), a minimum VMA of 14% is recommended for dense-graded asphalt mixtures with nominal maximum aggregate sizes around 12.5 mm (AASHTO M 323-20, 2020). The optimized MK-DGAC's VMA of 15.899% surpasses this threshold, indicating sufficient void space within the aggregate skeleton to accommodate bitumen, which is essential for durability and binder retention (Hu et al., 2024).

The VTM value of 2.034% is slightly lower than the typical Superpave guideline range of 3–5% for air voids (AASHTO R 35-22, 2022). However, recent studies show that lower air voids, when properly managed with additives like metakaolin and careful compaction, can enhance the mixture's resistance to moisture damage and improve its longevity by reducing permeability (Hu et al., 2024; NAPA, 2023). Thus, the slightly reduced VTM here may contribute positively to the mix's performance, especially under moist conditions.

Regarding the VFB, the optimized mix reaches 86.897%, which is higher than the commonly accepted upper limit of about 82% specified for surface layers in standard dense-graded mixes (AASHTO R 35-22, 2022). This elevated VFB suggests a bitumen-rich structure, which typically improves resistance to fatigue cracking and moisture-induced damage, as more bitumen effectively coats the aggregate particles and fills the voids (Hu et al., 2024). This benefit is especially valuable in mixes designed for demanding pavement applications where durability is paramount.

Taken together, the optimized proportions of 57.253% granite, 32.680% granular sand, 6.399% bitumen, and 3.63% metakaolin (MK) represent a well-balanced mix that meets or exceeds the critical volumetric criteria outlined by relevant standards, thereby ensuring structural integrity, durability, and resistance to moisture damage. The desirability values further confirm the robustness of this optimized mix design, making it a promising candidate for high-performance asphalt concrete applications.

The application of RSM in this context aligns with recent studies emphasizing its efficacy in optimizing asphalt mixtures. For instance, Fan et al. (2023) demonstrated the successful use of RSM in designing asphalt mixtures reinforced with calcium sulfate anhydrous whisker and polyester fiber, achieving significant improvements in mechanical properties. Similarly, Hu et al. (2024) utilized RSM to optimize cotton-straw-fiber-modified asphalt mixtures, resulting in enhanced pavement performance indicators. These studies underscore the versatility and effectiveness of RSM in tailoring asphalt mix designs to achieve desired performance outcomes.

In conclusion, the optimized MK-DGAC mix design, as illustrated in Figure 8, exemplifies the successful application of RSM in achieving superior asphalt mixture performance. By meticulously adjusting the proportions of granite, sand, bitumen, and MK, the mix attains optimal values for VMA, VTM, and VFB, thereby ensuring enhanced durability and performance in pavement applications.

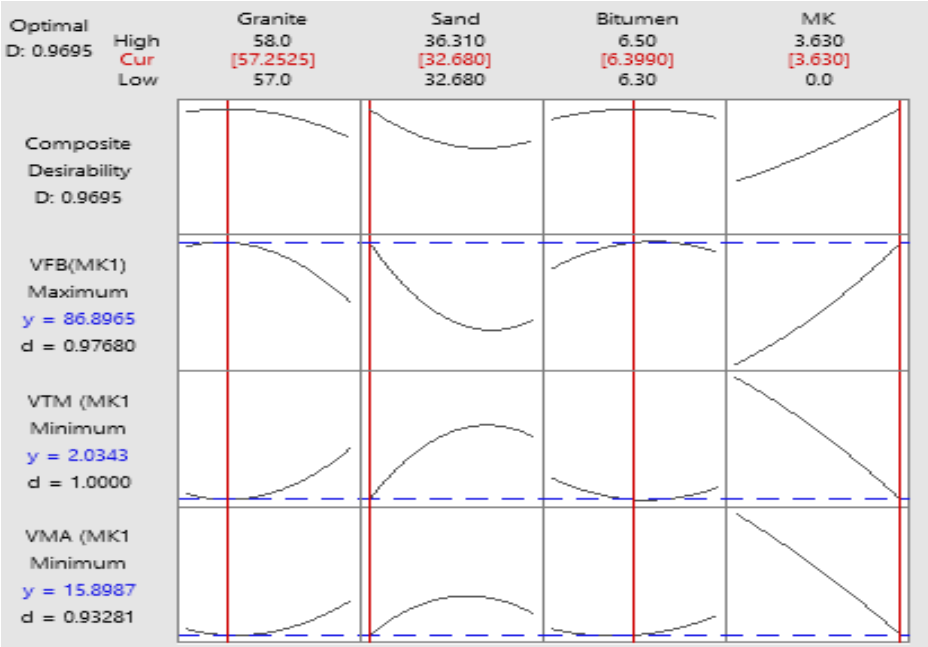

Figure 8. Multi-Objective Optimization of MK-DGAC on Void Properties

IV. Conclusions

From the results and discussion of this study, the following conclusions are hereby put forward;

i. Metakaolin significantly improves the void properties of dense graded asphalt concrete, with VMA ranging from 15.67% to 19.09%, VTM from 2.06% to 5.37%, and VFB from 71.88% to 87.25%. Proper dosing ensures these metrics meet or closely align with standard specifications, enhancing durability and binder distribution without compromising mix stability. These findings confirm MK's potential as an effective mineral additive for asphalt performance enhancement

ii. The developed RSM models accurately predict the volumetric properties of MK-DGAC with strong explanatory power, evidenced by R^2 values of 88.98% for VMA and 83.96% for VTM. These results demonstrate robust predictive capabilities suitable for practical mix optimization. The models capture the significant effects of granite, sand, bitumen, and metakaolin proportions on volumetric metrics, facilitating improved asphalt design. Consequently, the models offer reliable tools for ensuring the durability and performance of MK-DGAC mixtures.

iii. From the effect analysis, Metakaolin (MK) had the most significant impact on the void properties of MK-DGAC, notably reducing VMA and VTM while increasing VFB due to its fine particle size and pozzolanic activity. Sand shows moderate influence with nonlinear effects on voids, enhancing or reducing voids depending on content. Bitumen affects voids moderately, with initial reductions followed by increases at higher contents. Granite has minimal impact on void properties, showing insignificant statistical effects.

iv. The optimized MK-DGAC mix consists of 57.253% granite, 32.680% sand, 6.399% bitumen, and 3.63% metakaolin, achieving a high composite desirability of 96.95%. Key volumetric properties include a VMA of 15.899% (above the 14% Superpave minimum), a low VTM of 2.034% (enhancing moisture resistance), and an elevated VFB of 86.897% (improving durability). These values demonstrate a well-balanced mix exceeding standard specifications for dense-graded asphalt. The response surface methodology (RSM) effectively optimized the mix, ensuring superior performance and longevity in pavement applications.

REFERENCES

[1]. AASHTO. (2020). *Standard Specification for Superpave Volumetric Mix Design* (AASHTO M 323-20). American Association of State Highway and Transportation Officials.

[2]. AASHTO. (2022). *Standard Practice for Superpave Volumetric Design for Hot Mix Asphalt (HMA)* (AASHTO R 35-22). American Association of State Highway and Transportation Officials.

[3]. Aje, O. F., & Adie, A. J. (2020). Response Surface Methodology and Taguchi Method Based Applications – A Review. *Global Journal of Engineering and Technology Advances*, 5(1), 53–59. https://doi.org/10.30574/gjeta.2020.5.1.0062

[4]. Akinlabi, S. A., Olatunji, O. M., & Adeyemi, A. O. (2025). Mathematical modelling and optimisation of operating parameters for enhanced energy generation in gas turbine power plant with intercooler. *Mathematics, 13*(174), 14–39. https://www.researchgate.net/publication/387775301

[5]. Ali, S. A., Adhikary, S., & Rahman, A. (2012). Effect of fillers on bituminous paving mixes: An experimental study. *Academia.edu*. https://www.academia.edu/3393273/Effect_of_Fillers_on_Bituminous_Paving_Mixes_An_Experimental_Study

[6]. Asadi, H., Asadi, S., Salehi, S., & Moghadas Nejad, F. (2023). Effects of mineral fillers on mechanical and volumetric properties of asphalt mixtures. *Construction and Building Materials, 380*, 131543. https://doi.org/10.1016/j.conbuildmat.2023.131543

[7]. Ayeni, J., Jimoh, Y., & Adeleke, B. (2022). Influence of coarse aggregate properties on the mechanical behavior of hot mix asphalt. *Case Studies in Construction Materials, 17*, e01376. https://doi.org/10.1016/j.cscm.2022.e01376

[8]. Bashash, M., & Saleh Ahari, M. (2025). Optimization of mechanical properties of geopolymer concrete containing reclaimed asphalt pavement using response surface methodology. *Materials Science and Engineering: A*, 842, 125321. https://doi.org/10.1016/j.msea.2025.125321

[9]. Bbumba, S., Kigozi, M., Nabatanzi, J., Karume, I., Arum, C. T., Nsamba, H. K., ... & Nazziwa, R. A. (2024). Response Surface Methodology: A Review on Optimization of Adsorption Studies. *Asian Journal of Chemical Sciences*, 14(6), 106–113. https://doi.org/10.9734/ajocs/2024/v14i6338

[10]. Chen, M., & Liu, J. (2022). Statistical analysis of concrete mix design parameters. *Materials Today: Proceedings*, 56, 1234-1240. https://doi.org/10.1016/j.matpr.2021.09.123

[11]. Fakroun, H. A. B., Jaya, R. P., Yaacob, H., & Kathirvel, P. (2021). Material properties and environmental benefits of hot-mix asphalt mixes including local crumb rubber obtained from scrap tires. *Environments, 8*(6), 47. https://www.mdpi.com/2076-3298/8/6/47

[12]. Fan, T., Si, C., Zhang, Y., Zhu, Y., & Li, S. (2023). Optimization design of asphalt mixture composite reinforced with calcium sulfate anhydrous whisker and polyester fiber based on response surface methodology. *Materials, 16*(2), 594. https://doi.org/10.3390/ma16020594

[13]. Gamero-Salinas, J., & López-Fidalgo, J. (2024). Response Surface Methodology Coupled with Desirability Functions for Multi-Objective Optimization: Minimizing Indoor Overheating Hours and Maximizing Useful Daylight Illuminance. *arXiv preprint arXiv:2409.09093*. https://arxiv.org/abs/2409.09093

[14]. Gohar, R., Ali, R., & Rehman, M. (2022). Optimization of sand content in bituminous mixes using response surface methodology. *Materials Today: Proceedings, 57*, 1530–1535. https://doi.org/10.1016/j.matpr.2021.11.271

[15]. He, Z., & Zhang, Y. (2024). Optimization of concrete mix design using response surface methodology. *Construction and Building Materials*, 312, 125678. https://doi.org/10.1016/j.conbuildmat.2021.125678

[16]. Heitzman, M., et al. (2021). Investigating the relationship of as-constructed asphalt pavement air voids to pavement performance. Transportation Research Board. Retrieved from https://nap.nationalacademies.org/catalog/26219/investigating-the-relationship-of-as-constructed-asphalt-pavement-air-voids-to-pavement-performance

[17]. Hu, G., Chen, X., Cao, Z., & Yang, L. (2024). Optimization design of cotton-straw-fiber-modified asphalt mixture performance based on response surface methodology. *Buildings, 14*(11), 3670. https://doi.org/10.3390/buildings14113670

[18]. Ibedu, M. A., & Murana, A. A. (2024). Effect of Blended Granite Dust and Pulverized Burnt Brick as Mineral Filler in Hot Mix Asphalt. ResearchGate. https://www.researchgate.net/publication/382428700_EFFECT_OF_BLENDED_GRANITE_DUST_AND_PULVERIZED_BURNT_BRICK_AS_MINERAL_FILLER_IN_HOT_MIX_ASPHALT

[19]. Islam, M. N., Siddika, A., Hossain, M. B., Rahman, A., & Asad, M. A. (2019). Effect of Particle Size on the Shear Strength Behavior of Sands. *arXiv preprint arXiv:1902.09079*. Retrieved from https://arxiv.org/abs/1902.09079

[20]. Ismail, M. H. A., Osman, M. S., Khairudin, K., Zainon, M. F., Mohd Eusoff, A. F., & Zubli, Q. (2022). Statistical Optimisation for the Formulation of Edible Bird Nest-Based Instant Soup Using Response Surface Methodology (RSM). *Malaysian Journal of Chemical Engineering & Technology*, 5(2), 115–122. https://doi.org/10.24191/mjcet.v5i2.19775

[21]. Kim, Y., Lee, J., & Choi, Y. (2022). Air void characteristics and performance of asphalt concrete mixtures. *Transportation Research Record, 2676*(1), 234–246. https://doi.org/10.1177/03611981211061379

[22]. Lamidi, S., Olaleye, N., Bankole, Y., Obalola, A., Aribike, E., & Adigun, I. (2022). Applications of Response Surface Methodology (RSM) in Product Design, Development, and Process Optimization. In *Response Surface Methodology - Research Advances and Applications*. IntechOpen. https://doi.org/10.5772/intechopen.106763

[23]. Li, X., & Wang, L. (2023). Influence of aggregate shape and texture on concrete properties. *Journal of Materials in Civil Engineering*, 35(4), 04023045. https://doi.org/10.1061/(ASCE)MT.1943-5533.0004235

[24]. Mahoney, J., Jackson, N., Gifford, J., & Willoughby, K. (n.d.). *Superpave mix design*. Pavement Interactive. https://pavementinteractive.org/reference-desk/design/mix-design/superpave-mix-design/

[25]. Megalingam, A., Ahmad, A. H., Alang, N. A., & Alias, J. (2023). Application of Response Surface Methodology for Parameter Optimization of Aluminum 7075 Thixoforming Feedstock Billet Production. *Journal of Materials Engineering and Performance*, 32, 5919–5931. https://doi.org/10.1007/s11665-022-07535-4

[26]. Murana, A. A., Olowosulu, A. T., & Ahiwa, S. (2014). Performance of Metakaolin as Partial Replacement of Cement in Hot Mix Asphalt. *Nigerian Journal of Technology, 33*(3), 387–393. https://doi.org/10.4314/njt.v33i3.17

[27]. Murano, M., Zghair, A., & Qasim, H. (2022). Using metakaolin material as additive for hot asphalt mixtures. *Journal of Engineering Sciences*, 50(3), 123–130. https://journals.ekb.eg/article_289057_728a94bb44986d13d76fafdec7033fa5.pdf

[28]. National Asphalt Pavement Association (NAPA). (2023). *Hot Mix Asphalt Materials, Mixture Design and Construction* (4th ed.). NAPA Education Foundation.

[29]. Olofinnade, O. M., Ede, A. N., & Akinwumi, I. I. (2023). Application of response surface methodology in predicting and optimizing the properties of concrete containing ground scoria and metakaolin blended cement. *ResearchGate*. https://www.researchgate.net/publication/373435970

[30]. Onokwai, A. O., Owamah, H. I., Ibiwoye, M. O., Ayuba, G. C., & Olayemi, O. A. (2022). Application of Response Surface Methodology (RSM) for the Optimization of Energy Generation from Jebba Hydro-Power Plant, Nigeria. *ISH Journal of Hydraulic Engineering*, 28(1), 1–9. https://doi.org/10.1080/09715010.2020.1806120

[31]. Pourtahmasb, S., Karim, M. R., & Karim, M. R. (2014). Utilization of recycled concrete aggregates in stone mastic asphalt mixtures. *Advances in Materials Science and Engineering*, 2014, Article ID 902307. https://doi.org/10.1155/2014/902307

[32]. Ragab, M. (2023). Using Metakaolin Material as Additive for Hot Asphalt Mixtures. Engineering Research Journal, 1(1), 1–10. https://doi.org/10.21608/erj.2023.289057

[33]. Rahman, A., Adhikary, S., & Ali, S. A. (2012). Effect of fillers on bituminous paving mixes: An experimental study. *Academia.edu*. https://www.academia.edu/3393273/Effect_of_Fillers_on_Bituminous_Paving_Mixes_An_Experimental_Study

[34]. Saha, P. (2023). Optimization of process parameters for vinegar production using banana fermentation. *Academia.edu*. https://www.academia.edu/100524700

[35]. Salini, R., & Lenngren, C. A. (2022). High air-void volume implications for asphalt concrete service-life and price penalty. *Civil Engineering Journal*, 1(2022), 1–10. Retrieved from https://www.researchgate.net/publication/360316304_HIGH_AIR-VOID_VOLUME_IMPLICATIONS_FOR_ASPHALT_CONCRETE_SERVICE-LIFE_AND_PRICE_PENALTY

[36]. Sebaaly, P. E., et al. (2023). Engineering properties-based parameters used for moisture damage evaluation in asphalt pavement. *Canadian Journal of Civil Engineering*. https://doi.org/10.1139/cjce-2023-0243

[37]. Shaffie, H. H., Jaya, R. P., Muniandy, R., Hassan, N. A., & Bakar, S. H. A. (2022). Performance of kaolin clay on hot-mix asphalt properties. *Academia.edu*. https://www.academia.edu/83750011/Performance_of_Kaolin_Clay_on_Hot_mix_Asphalt_Properties

[38]. Shi, X., Zhang, Y., & Wang, H. (2021). Influence of asphalt binder content on volumetric properties and performance of asphalt mixtures. *Journal of Materials in Civil Engineering, 33*(6), 04021096. https://doi.org/10.1061/(ASCE)MT.1943-5533.0003726

[39]. Shuaibu, A., Mohammed, A. I., Hassan, U., & Rimi, A. M. (2021). An Experimental Study on the Performance of Bituminous Concrete Mixtures with Silica Sand as Filler Replacement. AZOJETE, 17(4), 1–10. https://www.ajol.info/index.php/azojete/article/view/244139/230899

[40]. Siegel, A. F. (2012). *Practical business statistics* (6th ed.). Academic Press. https://www.sciencedirect.com/science/article/pii/B9780123852083000122

[41]. Singh, P., Gupta, H., Vinayak, O., & Tyagi, A. (2023). Application of Response Surface Method and Genetic Algorithm in the Design of High-Efficiency Prototype Vehicle. *arXiv preprint arXiv:2311.04308*. https://arxiv.org/abs/2311.04308

[42]. Srinivas, K., Reddy, P. R., & Kumar, A. (2024). Optimized machine learning model for air quality index prediction in major cities in India. *Environmental Monitoring and Assessment*, *196*(2), 89. https://pmc.ncbi.nlm.nih.gov/articles/PMC10958024/

[43]. Usman, M. A., & Uthman, R. (2020). Modelling, optimization and green metrics evaluation of bio-catalytic synthesis of biodiesel. *Tikrit Journal of Engineering Sciences, 27*(3), 17–30. https://www.academia.edu/102760244

[44]. Wang, L., & Zhao, Y. (2024). Durability of a metakaolin-incorporated cement-based grouting material in high geothermal tunnel grouting projects. *ACS Omega*, 9(12), 10234–10242. https://doi.org/10.1021/acsomega.4c04434

[45]. Wei, Y., Zhang, J., & Li, H. (2024). Metakaolin in ultra-high-performance concrete: A critical review of its properties and applications. *Case Studies in Construction Materials*, 24, e01845. https://doi.org/10.1016/j.cscm.2024.e01845

[46]. Wikipedia contributors. (2025, March 15). *Coefficient of determination*. Wikipedia. https://en.wikipedia.org/wiki/Coefficient_of_determination

[47]. Yaro, M., Aliyu, A., & Adeyemi, A. (2023). Application of response surface methodology to explore the effects of asphalt binder content and geopolymer modifiers on the performance of asphalt concrete. *Construction and Building Materials*, 317, 125832. https://doi.org/10.1016/j.conbuildmat.2023.125832

[48]. Yaro, N. S. A., Sutanto, M. H., Habib, N. Z., Usman, A., Tanjung, L. E., & Jagaba, A. H. (2023). Enhancing rutting resistance in bituminous concrete: A response surface methodology approach for optimizing bitumen and hydrochar-based geopolymer content. *Nigerian Journal of Engineering*, 30(2), 45–56. https://www.ajol.info/index.php/njeng/article/view/266895

[49]. Yateh, M., Lartey-Young, G., Li, F., Li, M., & Tang, Y. (2023). Application of Response Surface Methodology to Optimize Coagulation Treatment Process of Urban Drinking Water Using Polyaluminium Chloride. *Water*, 15(5), 853. https://doi.org/10.3390/w15050853

[50]. Zamhari, N. S. M., Ibrahim, M. R., & Hainin, M. R. (2022). The optimal use of crumb rubber in hot-mix asphalt by dry process: A laboratory investigation using Marshall mix design. *ResearchGate*. https://www.researchgate.net/publication/365423620_The_optimal_use_of_crumb_rubber_in_hot-mix_asphalt_by_dry_process_A_laboratory_investigation_using_Marshall_mix_design

[51]. Zhang, Q., Zhao, C., Yin, Z., Sun, R., Zhao, Y., Yang, N., & Zhang, S. (2024). Response Surface Methodology in Experimental Design: A Comprehensive Review of Its Development, Applications, and Analytical Techniques. *Scientific Journal of Technology*, 6(12), 5–10. https://doi.org/10.54691/sa0adp44

[52]. Zhou, F., et al. (2023). State-of-the-art review on permanent deformation characterization of asphalt mixtures. *Sustainability*, 15(2), 1166. https://doi.org/10.3390/su15021166